Abstract
Comparison of ZnO nanoparticles and $ZnCl_2$ induced germ cell apoptosis in *Caenorhabditis elegans*
by Brittany O'Donnell
April, 2014
Director: Xiaoping Pan
DEPARTMENT OF BIOLOGY

There is inadequate research data available on manufactured ZnO nanoparticles. Manufactured nanoparticles are widely used in various products and production of manufactured nanoparticles is becoming increasingly abundant. Humans are exposed to ZnO nanoparticles in products such as sunscreen, toothpaste, and cosmetic products. Due to the frequent human contact with nanoparticles, such as ZnO, research on the resulting biological effects is highly significant. In this study, we utilized the model organism *Caenorhabditis elegan*s (*C. elegans*) to investigate the effects ZnO nanoparticle exposure can have on germ cell apoptosis and key genes involved in the apoptosis pathway. $ZnCl_2$ (Zn^{2+}) serves as a comparison of toxicity with ZnO nanoparticles in this study. It is known that ZnO nanoparticle exposure can have a severe effect on the reproduction process in *C. elegans*, however, it has yet to be tested whether or not ZnO nanoparticles affect germ cell apoptotic machinery as a possible mechanism of reproductive toxicity. Worms were exposed on an agar medium containing concentrations of ZnO nanoparticles and $ZnCl_2$ (range, 6.14×10^{-1}, 61.4, and 614 μM Zn). ZnO nanoparticles and $ZnCl_2$ both significantly increased the number of apoptotic cells as compared to the control in the 61.4 and 614 μM treatment groups ($p<0.05$). However, ZnO nanoparticles significantly induced nearly 2× more average apoptotic cells in the 61.4 μM treatment than the $ZnCl_2$ at the same concentration. This relationship was observed in both the bristol N2 wild type

(N2) and MD701 (bcIs39 [(lim-7)ced-1p::GFP + lin-15(+)]) strains. Genes involved in the apoptosis pathway (*ced-13, ced-3*, *ced-4*, *ced-9*, *cep-1, dpl-1*, *efl-1*, *efl-2*, *egl-1*, *egl-38*, *lin-35*, *pax-2*, and *sir-2.1)* were changed in response to ZnO nanoparticle exposure. *Cep-1*/p53 was significantly up-regulated in the 614 μM treatment ($p<0.05$). In the CEP-1 loss of function mutant, no significant increases were observed in germ cell apoptosis as compared to the control in any treatment group ($p>0.05$). Therefore, the increased apoptosis resulting from ZnO nanoparticle exposure is likely CEP-1 dependent. Following exposure, possible ZnO nanoparticles were observed in vivo in the worms using transmission electron microscopy, suggesting that the worms can possibly absorb the nanoparticles via various routes.

Comparison of ZnO nanoparticles and $ZnCl_2$ induced germ cell apoptosis in *Caenorhabditis elegans*

A Thesis

Presented To

The Faculty of the Department of Biology

East Carolina University

In Partial Fulfillment

of the Requirements for the Degree

Master of Science

by

Brittany O'Donnell

April, 2014

Comparison of ZnO nanoparticles and $ZnCl_2$ induced germ cell apoptosis in *Caenorhabditis elegans*

by

Brittany O'Donnell

APPROVED BY:

DIRECTOR OF DISSERTATION:_____
Xiaoping Pan, PhD

COMMITTEE MEMBER:_____
Baohong Zhang, PhD

COMMITTEE MEMBER:_____
Anthony Capehart, PhD

COMMITTEE MEMBER:_____
David Collier, PhD

CHAIR OF THE DEPARTMENT OF BIOLOGY:

_____
Jeff McKinnon, PhD

DEAN OF THE GRADUATE SCHOOL:

_____
Paul J. Gemperline, PhD

TABLE OF CONTENTS

LIST OF TABLES

LIST OF FIGURES

INTRODUCTION: PROJECT DESCRIPTION

Nature of the Problem

There is inadequate research data available on manufactured ZnO nanoparticles (NPs) and effects that could result from prolonged exposure on humans and other life forms. This is alarming due to the fact of how frequently humans are exposed to ZnO NPs and how increasingly abundant ZnO NPs are becoming in various products. My goal is to discover what potential consequences may arise in the future after such increasingly recurrent exposure to ZnO NPs.

Manufactured NPs are particles that have one or more dimensions of less than 100 nm (Wang, Wick, & Xing, 2009; SCENIHR (Scientific Committee on Emerging and Newly-Identified Health Risks), 21-22 June 2007). NPs are produced in metric tons per year and production is expected to increase over the next decade (Ma, Bertsch, Glenn, Kabengi, & Williams, 2009). In particular, ZnO NPs are used in products that most humans come into contact with on a daily basis such as, toothpaste, sunscreens, cosmetics or beauty products, and textiles (Wang et al., 2009). Due to expected increases of manufactured NPs and the frequency of human contact with NPs, research on biological effects of NPs like ZnO is of extreme importance. It is also important to understand how the safety and health of humans may be impacted as a result of prolonged exposure to ZnO NPs. The U.S. Environmental Protection Agency deemed nanoparticle research on both aquatic and terrestrial systems to be of future priority (U.S. Environmental Protection Agency, 2005 Office of Research and Development, Washington, DC).

Literature Review

There have been a few studies assessing the toxicological effects of manufactured ZnO NPs in the free living nematode *Caenorhabditis elegans* (*C. elegans*). One study compared the toxicological effects of manufactured ZnO NPs to that of $ZnCl_2$ (Ma et al., 2009). Endpoints evaluated were lethality, behavior (movement), reproduction. Four day old, wild-type N2 strain *C. elegans* were used for testing and maintained at 20°C. Average size of particles in the ZnO NP suspension used was determined to be 1.5 nm by transmission-electron microscopy. All metal solutions were made in buffered and unbuffered K-medium and all tests were performed in an aqueous medium. For the lethality test, worms were exposed to 5-6 concentrations of ZnO and $ZnCl_2$ (range, 325-1,625 mg Zn/L), for 24 hours. They found that as concentrations of Zn increased, mortality increased (10-100%), whereas mortality in control worms was less than 10% at all times (Ma et al., 2009). Concentrations used were fairly high (range, 325-1,625 mg Zn/L) and ZnO NPs were proven toxic. For movement or behavior, concentrations tested included 5-6 concentrations of ZnO and $ZnCl_2$ ranging from 50-1,000 mg Zn/L. Worms were exposed to these various concentrations for 4 hours at 20°C. Movement was tracked 1 hour after exposure by a video camera and computer equipped with tracking software. Average movement per worm per second was calculated using computer software. Control worms had an average movement speed of 3.5 μm per second. Results showed that for ZnO and $ZnCl_2$ movement responses occurred across one order of magnitude in concentration, from 100-20% of the control movement (Ma et al., 2009). To test reproductive effects a 72 hour assay was used, consisting of 5 concentrations of ZnO

NPs or $ZnCl_2$ ranging from 10-200 mg Zn/L, and a control. One adult worm was placed in each 1 ml of test solution for 72 hours of exposure. Following exposure, numbers of offspring were recorded. Average number of offspring in control was 122. A significant decrease in reproduction was observed as ZnO NP or $ZnCl_2$ concentration increased (10–200mg Zn/L). Also, when compared to lethality or movement, reproduction was affected at much lower concentrations. For reproduction, the concentration causing a 50% decrease in the number of offspring as compared to control was 46 mg Zn/L for ZnO NPs and 59 mg Zn/L for $ZnCl_2$ (Ma et al., 2009).

Authors proposed that ZnO NPs may have dissolved to Zn^{2+} in the test medium to activate toxicity (Ma et al., 2009). More testing will need to be done to test this theory. $ZnCl_2$ was found to be more toxic in the unbuffered than the buffered K-medium. This is due to the fact that free Zn^{2+} ions are the main cause of $ZnCl_2$ toxicity. Therefore, $ZnCl_2$ toxicity in the buffered K-medium decreased due to the decrease in free Zn^{2+} ion concentration, which in turn was caused by complexation of the Zn with other species in the solution (Ma et al., 2009). All resulting data from this study shows ZnO NP exposure to be toxic and resulting effects are significant. Therefore, toxicity of ZnO NPs should be further assessed.

Another study was also performed to determine whether metal oxide NPs were toxic to *C. elegans*. This study tested effects of ZnO NPs along with its bulk counterpart and reagent-grade $ZnCl_2$ (Wang et al., 2009). The stock suspensions of nanoparticulate and bulk ZnO used was 16.3 mg L^{-1}. Measured diameter of ZnO bulk particles was 532 nm. This study used wild type N2 strain of *C. elegans* at L1 stage. There were four

endpoints assessed which included lethality, length of worm, number of eggs inside the worm body and offspring per worm. Tested concentrations were 0.4, 0.8, 1.6, 4.1, 6.1 and 8.1 mg L^{-1} for nanoparticulate and bulk ZnO, and 0.7,1.4, 2.7, 6.8,10.2 and 13.6 mg L^{-1} for $ZnCl_2$ (Wang et al., 2009). Each test was carried out in ultrapure water. To test for lethality, approximately 30 L1 juveniles were transferred to petri plates containing various concentrations of tested particles along with a loopful of pelleted bacteria as food. Exposure lasted for 24 hours. Surviving worms were counted using a dissecting microscope. Results showed that LC50 values (lethal concentration at which 50 percent of the organisms die during testing) calculated were, respectively, 2.2, 2.3 and 2.9 mg L^{-1} for nanoparticulate and bulk ZnO and $ZnCl_2$ (Wang et al., 2009). ZnO NPs, caused lethality when exposed for 24 hours. It is also notable that the ZnO NP concentrations tested were considerably low and yet still caused lethality. To test both growth and reproductive effects, L1 worms were exposed under the same conditions as lethality test worms, these worms were exposed for 5 days as opposed to 24 hours (Wang et al., 2009).

Results revealed that exposure to 1.6 mg L^{-1} and 4.1 mg L^{-1} for both ZnO NPs and bulk ZnO significantly reduced the growth of *C. elegans*, number of eggs inside the worm and offspring per worm. Effect on growth and number of eggs inside the worm was not significantly different between ZnO NPs, bulk ZnO and $ZnCl_2$. However, the number of offspring per worm exposed to ZnO NPs was significantly less than that of the bulk ZnO at 0.8 and 1.6 mg L^{-1} (Wang et al., 2009). These experiments were carried out in the dark, therefore, production of reactive oxygen species (ROS) were probably a minimal cause of toxicity. According to this study, effects seen by ZnO NPs could have

been partly caused by the release of dissolved Zn^{2+}. It could not fully be determined that toxicity of the nanoparticles was caused by dissolved Zn^{2+} alone and there may be a nanoparticle-specific toxic mechanism (Wang et al., 2009). These results support the fact that more research on ZnO NPs is necessary because ZnO NPs have a significant negative impact on the *C. elegans* reproduction. It is obvious that NPs are toxic and exposure to NPs should be kept to a minimum if possible, especially with NPs such as ZnO, because even with exposure to low concentrations of ZnO NPs, harmful effects are evident.

An additional study examined toxicity of ZnO NPs at environmentally relevant concentrations in *C. elegans* (Wu et al., 2013). NPs used were 30 nm in size and each test involved prolonged exposure of the *C. elegans* from the L1 stage to adult (approximately 3 days). Endpoints assessed were lethality, growth, locomotion/behavior, and reproduction. Stock suspension concentrations were prepared in K medium and concentrations of the metal oxide NPs used were 0.0005, 0.005, 0.05, 0.5, 5, 10, and 50 μg/L. *C. elegans* used were of the N2 wild type strain. Tests were carried out in 12-well sterile tissue culture plates in the presence of food (Wu et al., 2013).

Results for the lethality test revealed that prolonged exposure (L1-adult) to 50 μg/L of ZnO NPs significantly increased the mortality of the worms. Survival was not obviously affected with prolonged exposure to 0.0005-10 μg/L ZnO NPs. Results for the growth test, which were determined by length of worm, were found to be exactly the same as the results of the lethality test. No affect was seen with prolonged exposure to 0.0005-10 μg/L of the examined metal oxide NP. However, when exposed to 50 μg/L

ZnO NPs, body lengths of the worms were significantly shortened. Reproduction toxicity effects were assessed using brood size as an endpoint. Prolonged exposure to 0.0005-0.05 μg/L ZnO NPs did not affect brood size of the worms. Prolonged exposure to 0.5–50 μg/L ZnO NPs significantly decreased brood size of nematodes compared to control. Prolonged exposure to 0.05–50 μg/L of ZnO NPs caused a significant decrease in the number of head thrashes and body bends of worms compared to control. Finally, prolonged exposure to 0.0005–0.005 μg/L of ZnO NPs did not affect the behavior of the worms. In all endpoints assessed including lethality, growth, reproduction, and behavior, ZnO NPs were proven to be most toxic and caused the most significant effects (Wu et al., 2013). This study suggests that oxidative stress is one mechanism behind toxicity of ZnO NPs. This was confirmed by a reactive oxygen species (ROS) production assay. It was found that ROS production was significantly correlated with lethality, growth, reproduction, body bends and head thrashes. To further confirm that oxidative stress induced toxicity, they treated ZnO NP exposed worms with antioxidants (10 mM ascorbate). Post-treatment of antioxidants after prolonged exposure to 50 μg/L ZnO NP, significantly suppressed increases in mortality, decreases in body length, body bends, and head thrashes, reduction in brood size, and the induction of ROS production (Wu et al., 2013). Interestingly, this study (Wu et al., 2013) used environmentally relevant concentrations. Thus, even at concentrations which are environmentally relevant, ZnO NPs cause adverse effects.

Data and results provided by research that has been done so far involving ZnO NPs and *C. elegans* is alarming and draws concern. All literature reviewed indicates that

exposure to ZnO NPs at various concentrations, including environmentally relevant concentrations can have consequences in *C. elegans*. When compared to the control, effects of ZnO NP exposure included increased mortality, decreased number of offspring produced, decreased number of eggs inside the body, reduction in body length, and decrease in the number of body bends and head thrashes. ZnO NPs have toxic effects and are harmful to organisms when they are exposed for a prolonged period of time. Production of manufactured ZnO NPs is escalating and this trend is expected to continue (Ma et al., 2009). With humans being exposed daily to ZnO NPs in products such as toothpaste, sunscreen, cosmetics, and textiles, more research on ZnO NPs needs to take place.

Therefore, it is of importance to reveal effects as well as underlying toxicity mechanisms of ZnO NPs so that the manufacture and use of these NPs can be regulated accordingly. Recently *C. elegan* studies using ZnO NPs have assessed endpoints such as lethality, growth, reproduction, and behavior for toxicological evaluation. These studies described above indicate ZnO NPs cause a reduction in offspring and the number of eggs (Ma et al., 2009; Wang et al., 2009; Wu et al., 2013). However, to my knowledge, no one has yet to test whether or not ZnO NPs affect germ cell apoptotic machinery (programmed cell death) as a mechanism of reproductive toxicity.

Hypothesis

I hypothesize that exposure to ZnO NPs will lead to increased germ cell apoptosis, induce more apoptosis than Zn^{2+} ($ZnCl_2$), and affect key genes in the apoptosis pathway.

Objectives

- Evaluate effects of $ZnCl_2$ and ZnO NP exposure on germ cell apoptosis in *Caenorhabditis elegans*
- Determine effects of $ZnCl_2$ and ZnO NP exposure on expression of genes involved in the apoptosis pathway

METHODS/MATERIALS

Organism

Caenorhabditis elegans are free-living nematodes found in aqueous environment of soil ecosystems and play a key role in nutrient cycling (Wang et al., 2009; Wu et al., 2013). They are ideal model organisms because their complete genome has been sequenced, they have 60-80% homology with the human genome, a short life cycle (approximately 3 days), and life span (approximately 2-3 weeks), and are also easily cultured and maintained. Due to their translucent bodies, developmental processes, such as the stage of growth, and number of eggs inside the body, can be easily monitored via microscope (Fig. 1). As a food source, *C. elegans* use *Escherichia coli* (*E. coli* OP50), which is easily cultured. *C. elegans* are used as great models for toxicological studies for an extensive variety of environmental toxicants (Leung et al., 2008). Recently there have been a few studies evaluating the toxicity of various NPs including ZnO NPs on *C.*

elegans (Ma et al., 2009; Ma et al., 2011; Wang et al., 2009; Wu et al., 2013). The life cycle of *C. elegans* consists of four larval stages (L1-L4) before reaching adult stage (Fig. 2). Due to the high level of conserved genes and gene pathways from *C. elegans* to humans, data collected in *C. elegans* studies can be indicative for higher organisms. *C. elegans* can be hermaphrodites, males, and females, therefore they can self- or cross-fertilize.

In this study 3 strains of *C. elegans* were used: Bristol N2 wild type (N2), MD701 (bcIs39 [(lim-7)ced-1p::GFP + lin-15(+)]), and TJ1(cep-1(gk138) I). N2 hermaphrodites were used to ensure that worms and their offspring are genetically identical. The MD701 strain allows visualization of apoptotic cells. The *ced-1* gene is involved in apoptosis. This gene was upregulated when germ cells undergo apoptosis, working as a signal to promote the engulfment of cell corpses by phagocytic sheath cells. As CED-1 expresses on the cell membrane, apoptotic cells can be visualized as a green fluorescent circle in the loop region of the MD701 gonad (Gartner, Boag, & Blackwell, 2008). The TJ1 strain is a CEP-1 loss of function mutant used to determine if CEP-1 is needed in the ZnO NP induced apoptosis.

Germline Apoptosis

There are 2 categories of *C. elegans* germline apoptosis. During normal oogenesis many early germ cells undergo apoptosis. This process is significant to the reproductive process and is broadly conserved from worms to mammals. Nearly 50% of predetermined oocytes undergo apoptosis under normal conditions. These cells serve as a population of nurturing cells, providing mature oocytes with cytoplasmic components

(Gartner et al., 2008; Gumienny, Lambie, Hartwieg, Horvitz, & Hengartner, 1999; Hall & Altun, 2008). Once the nurse cells have been utilized apoptosis is activated producing a nurse cell corpse which is engulfed by neighboring somatic gonad sheath cells (Fig. 3a) (Gumienny et al., 1999). The second category is germline apoptosis induced by environmental stressors such as DNA damage or pathogenic infection. Environmental stress can cause a significant increase in apoptosis as compared to the normal range. The reproductive process can be severely affected by such increases in apoptosis, reducing the number of mature oocytes and thus reducing the number of offspring (Ruan et al., 2012). Apoptosis normally occurs within the transitional region (mitosis to meiosis) or gonadal loop (Fig. 3a). As genetically unsuitable cells pass through the gonad loop or death zone they undergo apoptosis to prevent further maturation into oocytes (Hengartner, 1997). Normally, in wild type *C. elegans* hermaphrodites, approximately 150 germ cells will undergo programmed cell death but only 0-3 corpses will be observed any time throughout the first 3-4 days of adulthood (Gumienny et al., 1999).

Apoptosis Pathway

Many genes involved in the main apoptosis pathway have human homologs (fig. 3b) (Hengartner, 1997). *Cep-1* promotes DNA damage-induced apoptosis (WormBase, a). This gene increases transcription of *egl-1* and *ced-13* which are both similar to BH3 (Bcl-2 homology domain) in mammals, cell death activators. Both EGL-1 and CED-13 interact directly with CED-9, an anti-apoptotic protein, which encodes for the cell death inhibitor *Bcl-2* in mammals, and inhibit its transcription, inducing the release of CED-4 and causing activation of CED-3 (caspase). *Ced-4* encodes for a protein similar to Apaf-1

in humans and regulates *ced-3* activity which is required for carrying out apoptosis (WormBase, b; WormBase, c). *Lin-35* encodes for Rb, the retinoblastoma protein, and promotes physiological apoptosis by inhibiting transcription of *ced-9* (Gartner et al., 2008). PAX-2 and EGL-38 are Pax-family proteins that work to suppress the apoptosis by increasing transcription of *ced-9* (Gartner et al., 2008). *Dpl-1* encodes for DP (protein transcription factor) in mammals and works along with *efl-1/2*, which encodes for the transcription factor E2F in mammals. DPL-1, Rb, and E2F seem to work together to increase CED-4 and CED-3, therefore promoting germ cell apoptosis (Gartner et al., 2008) (Table 1).

Fig. 1. Translucent body, clearly showing internal egg hatching (arrows). This indicates the outside environment is stressful.

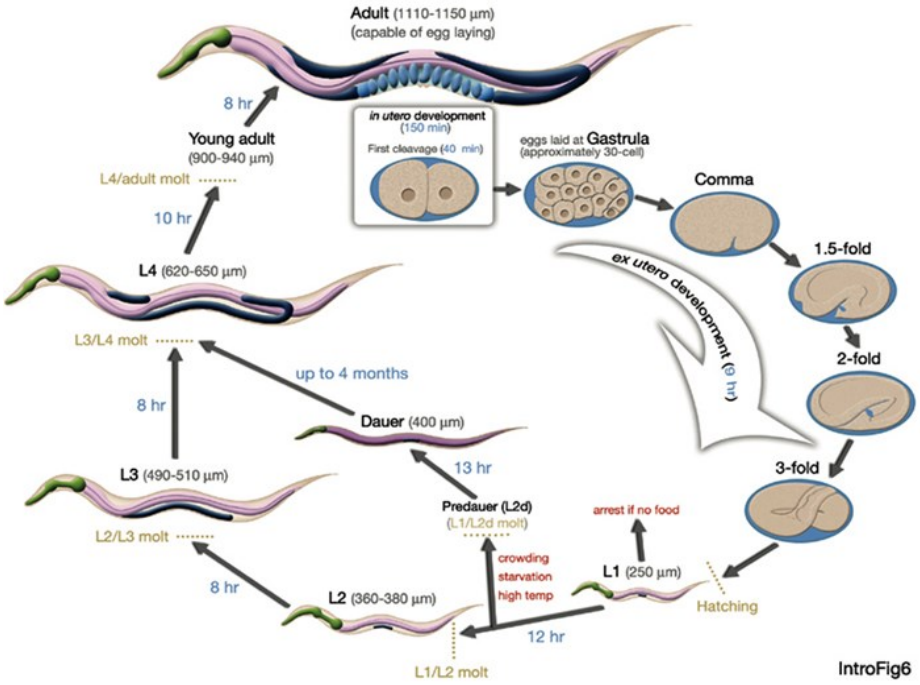

Fig 2. Life cycle of *C. elegans*
http://www.wormatlas.org/ver1/handbook/anatomyintro/anatomyintro.htm

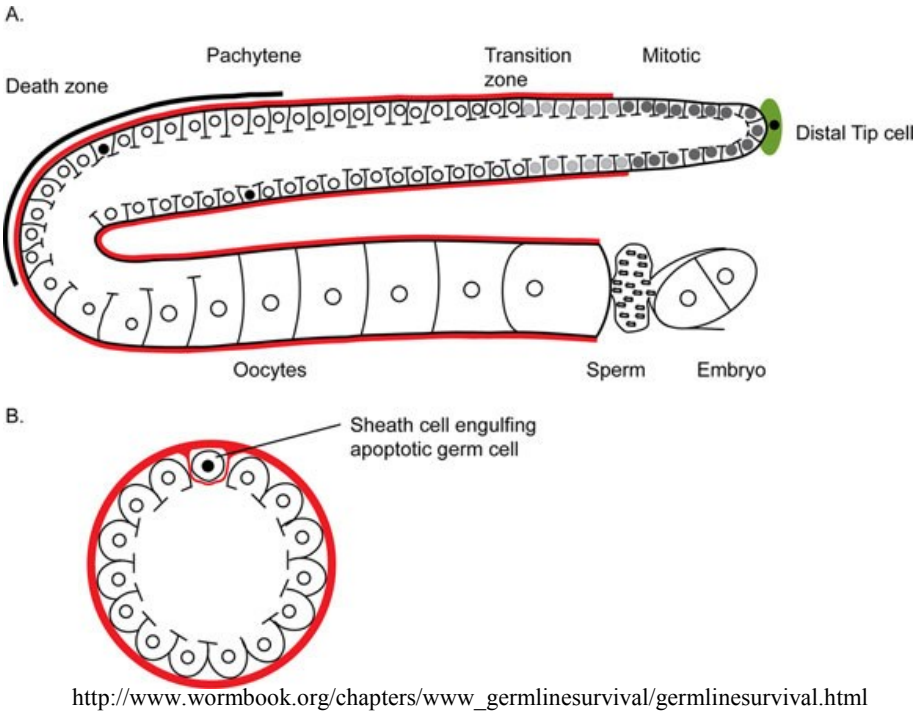

http://www.wormbook.org/chapters/www_germlinesurvival/germlinesurvival.html

Fig. 3a. Gonad arm and germline apoptosis. A) Gonad arm of adult hermaphrodite. B) Cross section of loop region showing apoptotic cell being engulfed by sheath cell (Gartner et al., 2008).

Table 1: Description of 13 genes involved in the apoptosis pathway

Gene Symbol	Locus Tag	Gene Description	Function	Reference
ced-3	C48D1.2	CEll Death abnormality	caspase protein and initiates apoptosis	(Bailly & Gartner, 2013; Denning, Hatch, & Horvitz, 2013)
ced-4	C35D10.9	CEll Death abnormality	Apaf-1 homolog	(Pourkarimi, Greiss, & Gartner, 2012; Zou, Henzel, Liu, Lutschg, & Wang, 1997)
ced-9	T07C4.8	CEll Death abnormality	Bcl-2 homolog; mitochondrial fusion and fission; inhibits apoptosis	(Pourkarimi et al., 2012)
ced-13	R09F10.9	CEll Death abnormality	BH3-only domain	(Schumacher et al., 2005)
cep-1	F52B5.5	C. Elegans P-53-like protein	p53 tumor suppressor	(Derry, Putzke, & Rothman, 2001)
dpl-1	T23G7.1	vertebrate transcription factor DP-Like	DP ortholog	(Ceol & Horvitz, 2001; Chi & Reinke, 2009)
efl-1	Y102A5C.18	E2F-like (mammalian transcription factor)	E2F homolog	(Brodigan, Liu, Park, Kipreos, & Krause, 2003)
efl-2	Y48C3A.17	E2F-LIKE (mammalian transcription factor)	E2F homolog	(Boxem & van den Heuvel, 2002)
egl-1	F23B12.9	EGg Laying defective	BH3-only domain	(Schumacher et al., 2005)
egl-38	C04G2.7	EGg Laying defective	encodes a protein part of the same family as pax-2,5,8; required for cell fate in hermaphrodites	(Chamberlin et al., 1997)
lin-35	C32F10.2	abnormal cell LINeage	Retinoblastoma (Rb) ortholog	(Ceol & Horvitz, 2001)
pax-2	K06B9.5	PAX (Paired box) transcription factor	transcription factor	(Park, Jia, Rajakumar, & Chamberlin, 2006)
sir-2.1	R11A8.4	yeast SIR related	aging and lifespan	(Kenyon, 2010; Ludewig et al., 2013)

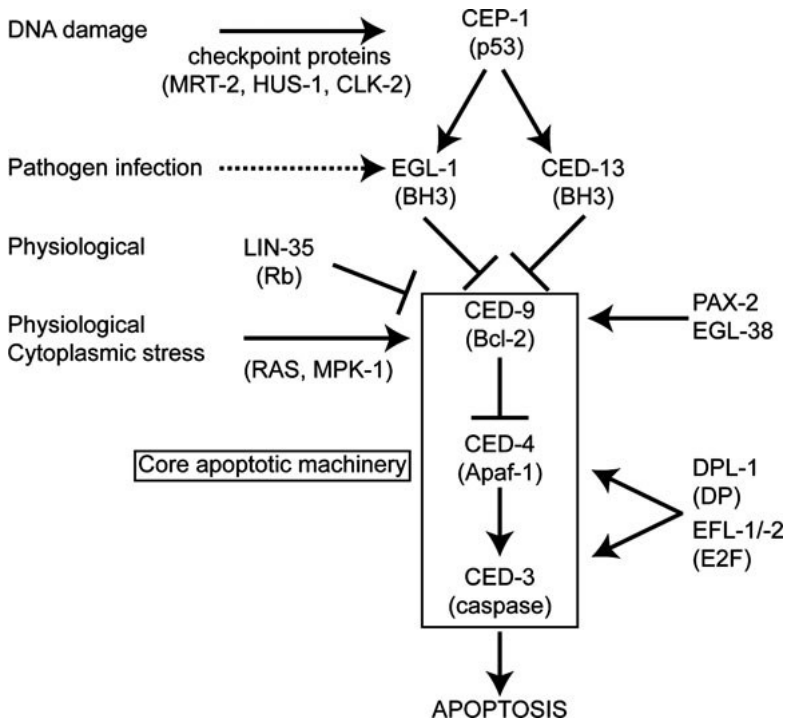

http://www.wormbook.org/chapters/www_germlinesurvival/germlinesurvival.html

Fig. 3b. Apoptosis pathway. Includes core apoptotic components (CED-9, CED-4, CED-3). In parenthesis are the human homologs that correspond with the *C. elegans* genes (Gartner et al., 2008).

Fig. 4. Magnified image of eggs (brackets) inside the body of *C. elegans*. Worms will be lysed and eggs will be released.

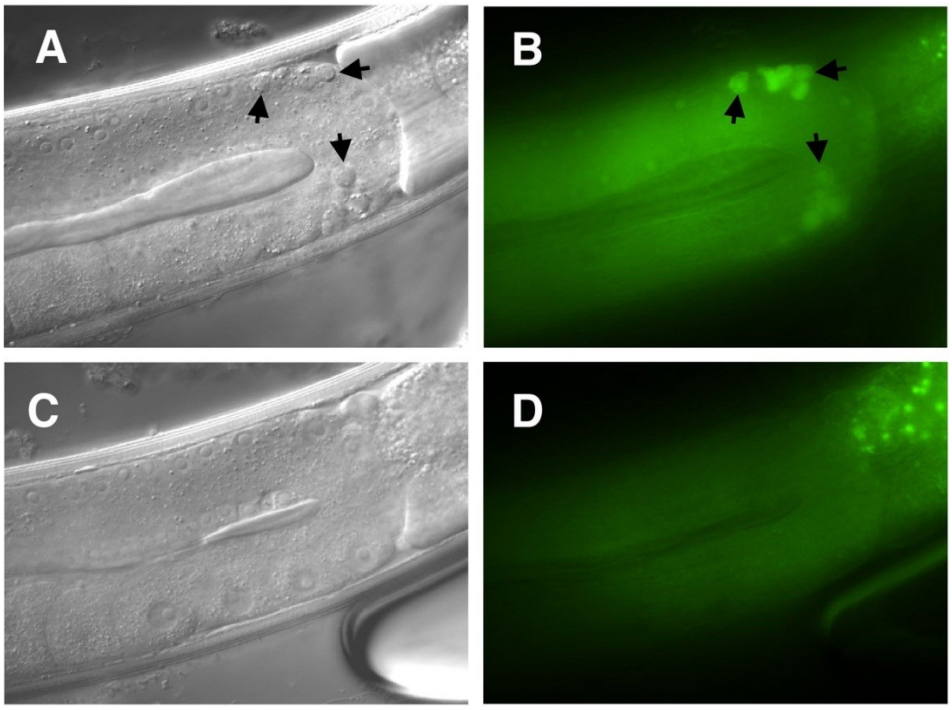

Fig. 5. Arrows indicate apoptotic cells. A. and C. show gonad arms without fluorescence. B. and D. show gonad arms with fluorescence after SYTO 12 assay (Shaham & ed., January 2, 2006).

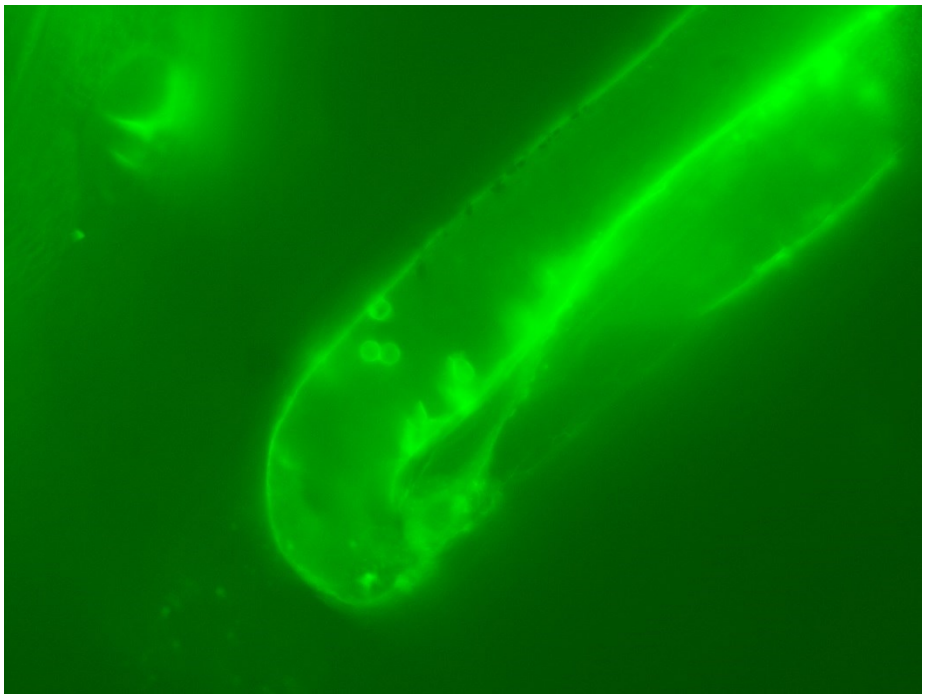

Fig. 6. Gonad arm of *C. elegan* with apoptotic cells (green fluorescent circles). MD701 strain

Statistical Analysis

For statistical analysis, the IBM SPSS Statistics 20 software for Windows 7 was used. To determine statistical differences between treatment and control groups in apoptosis cell counts and gene expression fold changes the statistical test analysis of variance (ANOVA) was used. If treatment groups were statistically significant at $p < 0.05$ level, least significant difference (LSD) multiple comparisons were carried out to compare means among groups.

Project Relevance

Uncovering possible damaging effects that human exposure to ZnO NPs could have in the future would yield great contributions to the medical field, the environment, and to the public. Being that *C. elegans* have 60-80% homology with the human genome, findings will be useful for human extrapolations. Metal oxide NPs are not biodegradable and consequences of this are not known (Wang et al., 2009). Therefore, this study is also significant to environmental organisms including terrestrial and aquatic animals. It will also provide evidence of harmful effects of NPs which will help agencies, such as the Environmental Protection Agency, better regulate production of NPs such as ZnO NPs.

RESULTS

MD701 (bcIs39 [(lim-7)ced-1p::GFP + lin-15(+)]) strain

ZnO NP worms had an average of 1.5, 4.3, and 2.7 engulfments for the control, 61.4 μM, and 614 μM treatments, respectively. $ZnCl_2$ worms had an average of 1.4, 2.5, and 2.6 engulfments for the control, 61.4 μM, and 614 μM treatments, respectively. Both

the 61.4 and 614 µM groups for ZnO NP and $ZnCl_2$ were found to be statistically significant from the control. ZnO NP 61.4 µM concentration significantly induced more apoptosis than the 614 µM ZnO NP concentration. Also apoptosis in this concentration was significantly increased compared to the $ZnCl_2$ 61.4 and 614 µM groups (Fig. 7, 8). Results indicate, based on the 61.4 µM ZnO NP group, that ZnO NPs are more potent than free Zn^{2+} ($ZnCl_2$), in terms of apoptosis induction at specific concentrations.

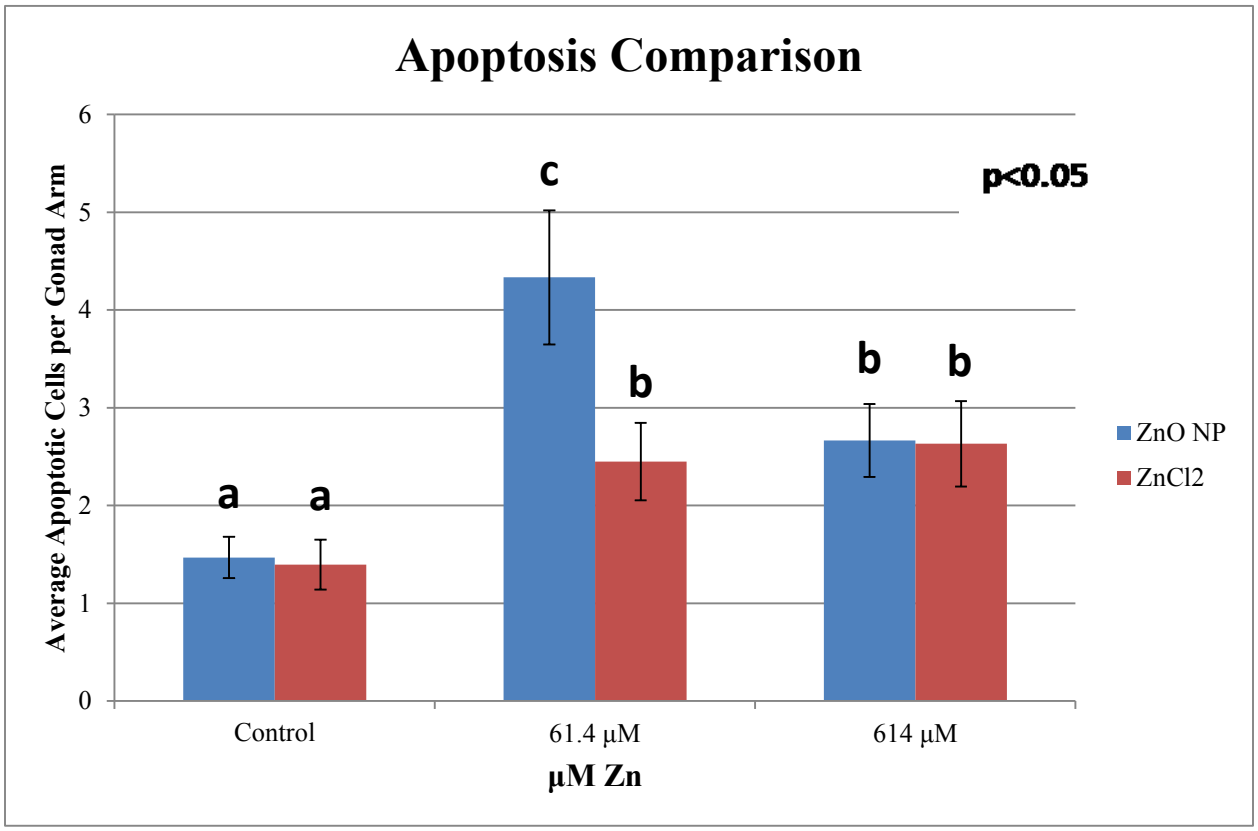

Fig. 7. Average number of engulfments per gonad arm after L1-adult dose (72 hrs). MD701 (bcIs39 [(lim-7)ced-1p::GFP + lin-15(+)]) strain. Different letters denote statistically significant differences. Error bars indicate standard deviations of 3 individual experiments (each consisting of 10 worms).

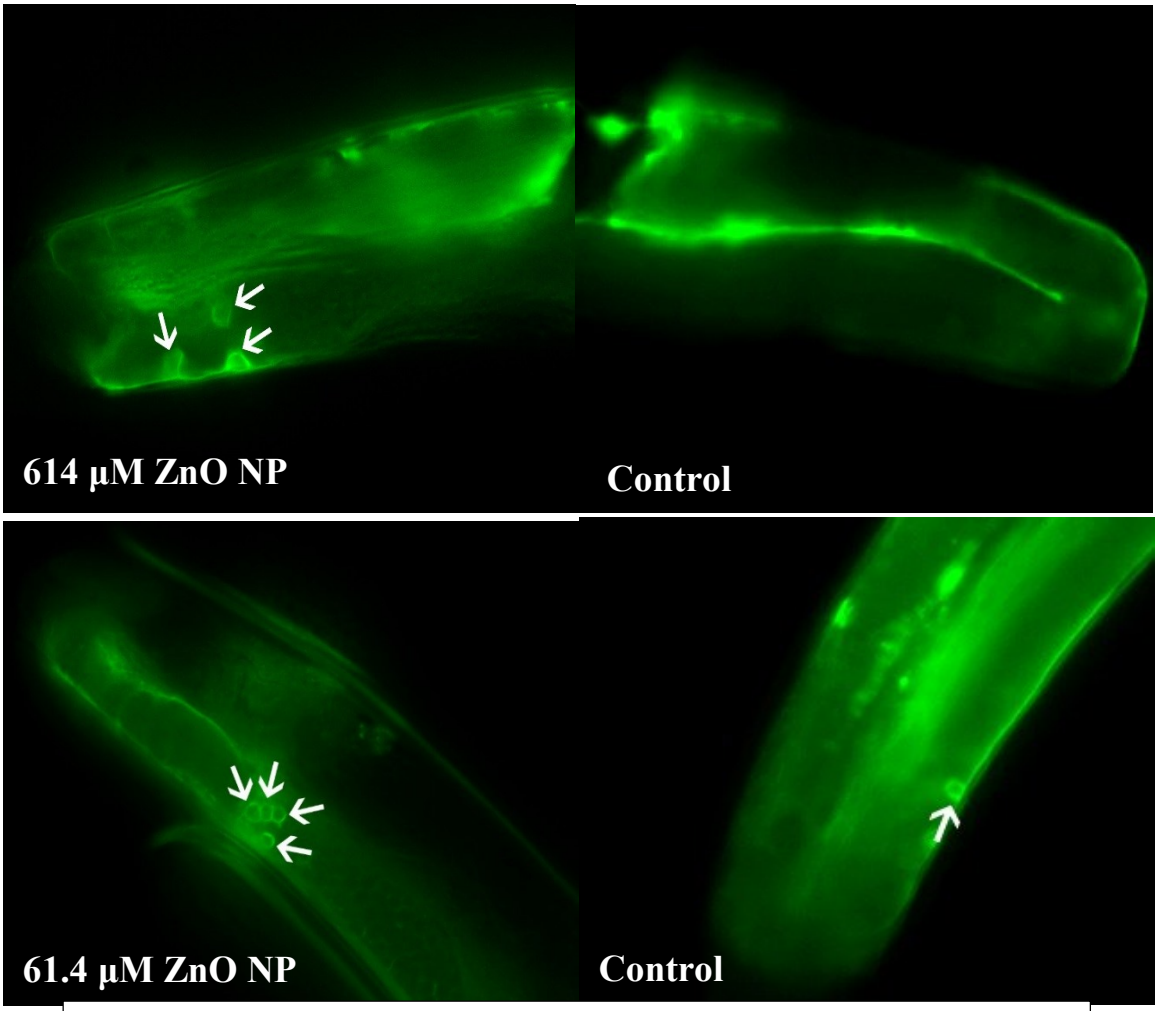

Fig. 8. ZnO NP 72 hr dose. Apoptotic cells appear as green fluorescent circles indicated by white arrows. MD701 (bcIs39 [(lim-7)ced-1p::GFP + lin-15(+)]) strain.

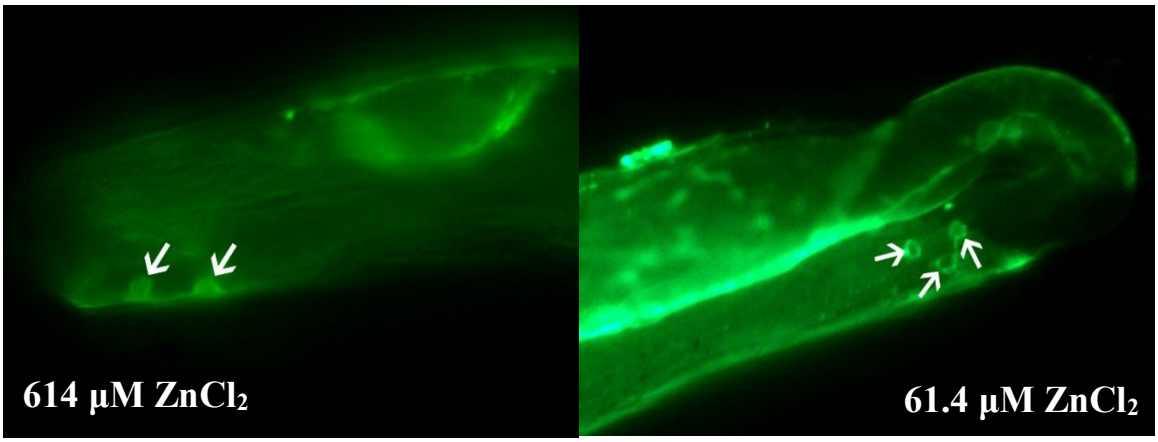

Fig. 9. $ZnCl_2$ 72 hr dose. Apoptotic cells appear as green fluorescent circles indicated by white arrows. MD701 (bcIs39 [(lim-7)ced-1p::GFP + lin-15(+)]) strain.

SYTO 12 Assay on N2 worms

ZnO NP treated N2 worms had an average of 1.6, 1.7, 4.6, and 2.8 apoptotic cells for the control, 6.14×10^{-1} μM, 61.4 μM, and 614 μM treatments, respectively. The 6.14×10^{-1} μM group showed no significant difference compared to control. The 61.4 and 614 μM treatments significantly increased the number of apoptotic cells as compared to control. The number of apoptotic cells in the 61.4 μM group was significantly higher than the 614 μM treatment group ($p<0.05$). These results are comparable to the findings using the MD701 strain, i.e. the wild-type N2 worms subjected to the SYTO 12 assay displayed approximately the same average number of apoptotic cells in all groups as in MD701 strain worms (Fig. 10, 11). $ZnCl_2$ N2 worms had an average of 1.6, 1.6, 2.4, and 2.5 apoptotic cells for the control, 6.14×10^{-1} μM, 61.4 μM, and 614 μM treatments, respectively. The 6.14×10^{-1} μM group showed no significant difference compared to control, the 61.4 and 614 μM treatments significantly increased the number of apoptotic cells as compared to control. Unlike the ZnO NP treatments, no significant difference was found between the 61.4 and 614 μM treatments (Fig. 10, 12).

Comparing the ZnO NP treatments to the $ZnCl_2$ treatments, no significant difference was found between the controls or the 614 μM treatment groups. However, apoptosis in the 61.4 μM ZnO treatment group was significantly higher than apoptosis in the 61.4 μM $ZnCl_2$ treatment group. To determine if the observed increases in apoptosis from the ZnO NPs is CEP-1/p53 dependent, we performed the experiment using the *TJ1(cep-1(gk138) I) strain.* The CEP-1/p53 mutant worms had averages of 1.6, 1.6, 2, and 1.7 apoptotic cells per gonad arm for the control, 6.14×10^{-1} μM, 61.4 μM, and 614

µM ZnO NP treatments, respectively. Results showed no statistically significant differences between groups ($p>0.05$). Findings suggest that observed apoptosis follows a CEP-1/p53 dependent pathway, as the number of apoptotic cells showed no increase in the CEP-1/p53 mutant strain (Fig. 13, 14).

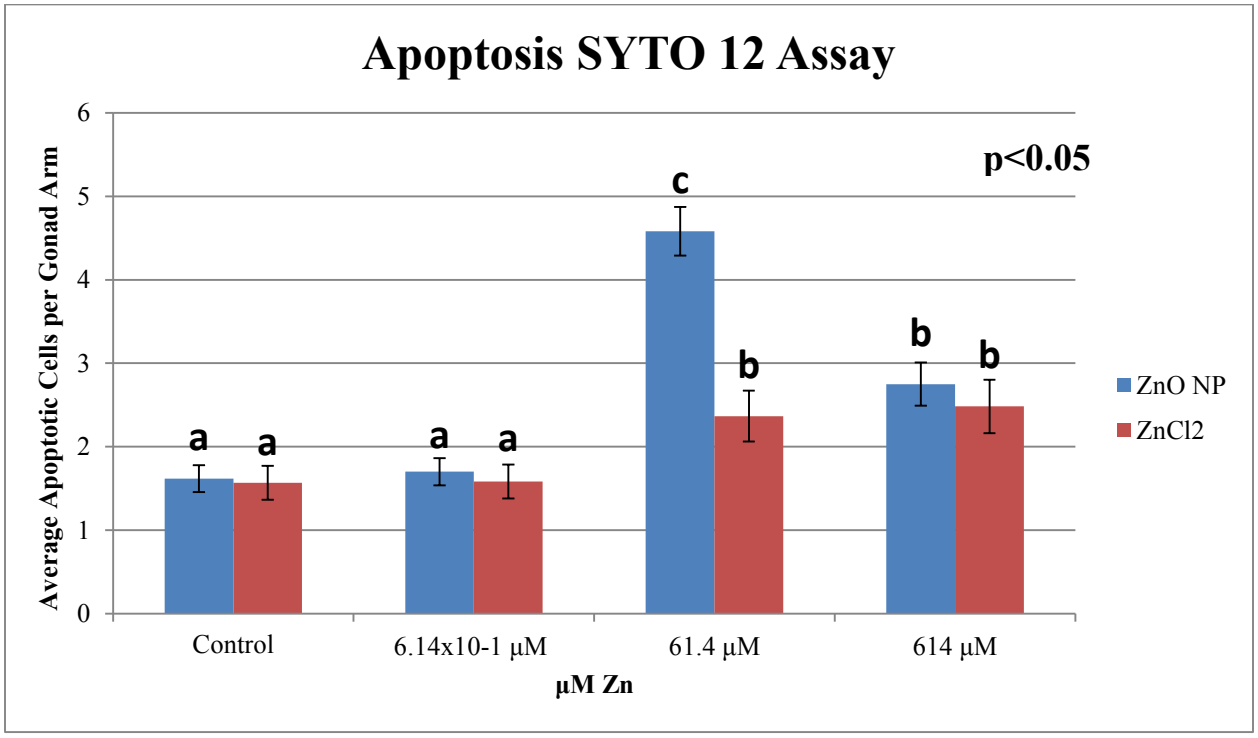

Fig. 10. Average number of apoptotic cells per gonad arm after L1-adult stage (72 hrs) dosing. SYTO 12 staining N2 strain. Different letters denote statistically significant differences. Error bars indicate standard deviations of 3 individual experiments (each consisting of 10 worms).

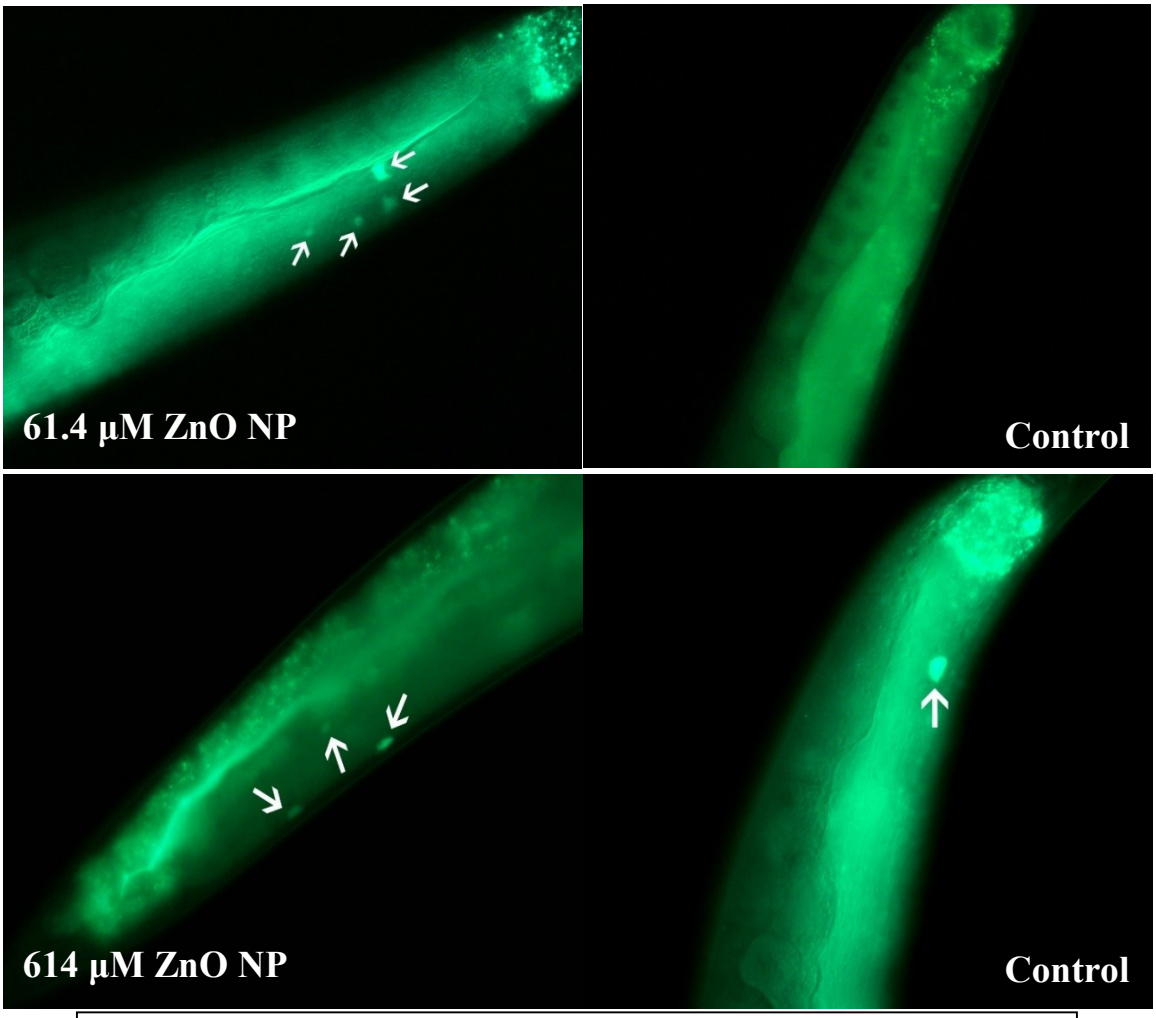

Fig. 11. ZnO NP (72 hr dose). SYTO 12 assay. Apoptotic cells appear as solid green dots indicated by white arrows.

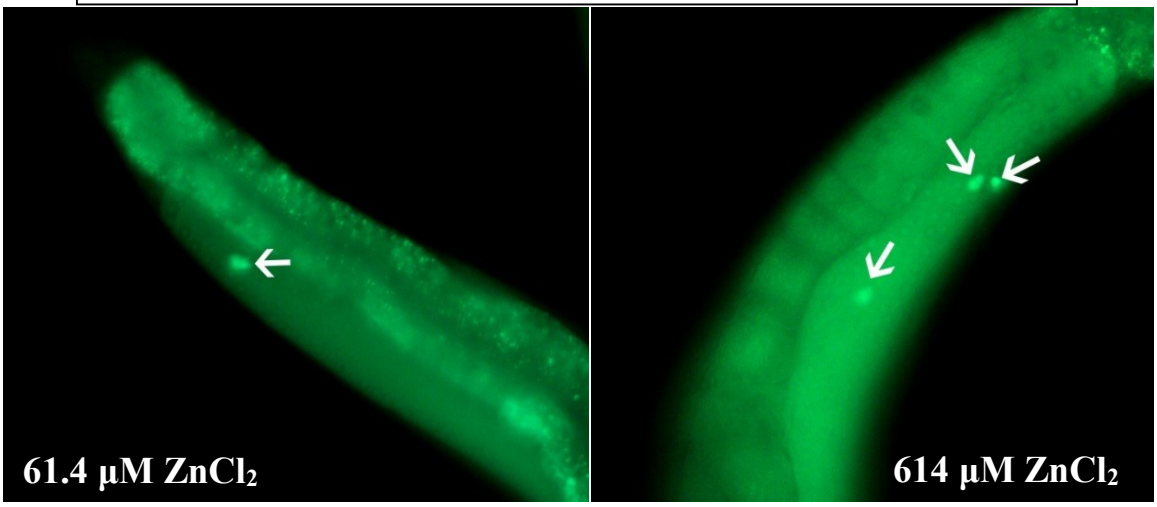

Fig. 12. $ZnCl_2$ (72 hr dose). SYTO 12 assay. Apoptotic cells appear as solid green dots indicated by white arrows.

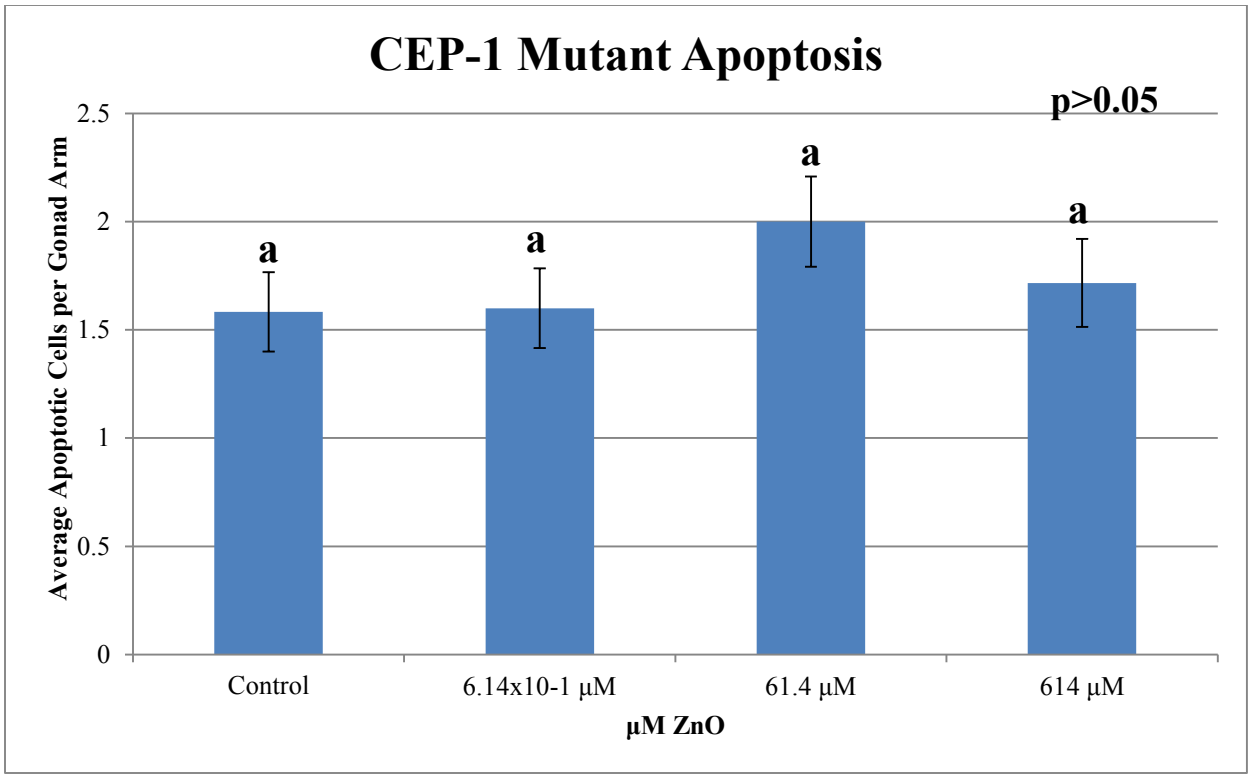

Fig. 13. Average number of apoptotic cells per gonad arm after L1-adult stage (72 hrs) dosing. (SYTO 12) TJ1 strain. Different letters denote statistically significant differences. Error bars indicate standard deviations of 3 individual experiments (each consisting of 10 worms). No significant difference among control or any of the treatments.

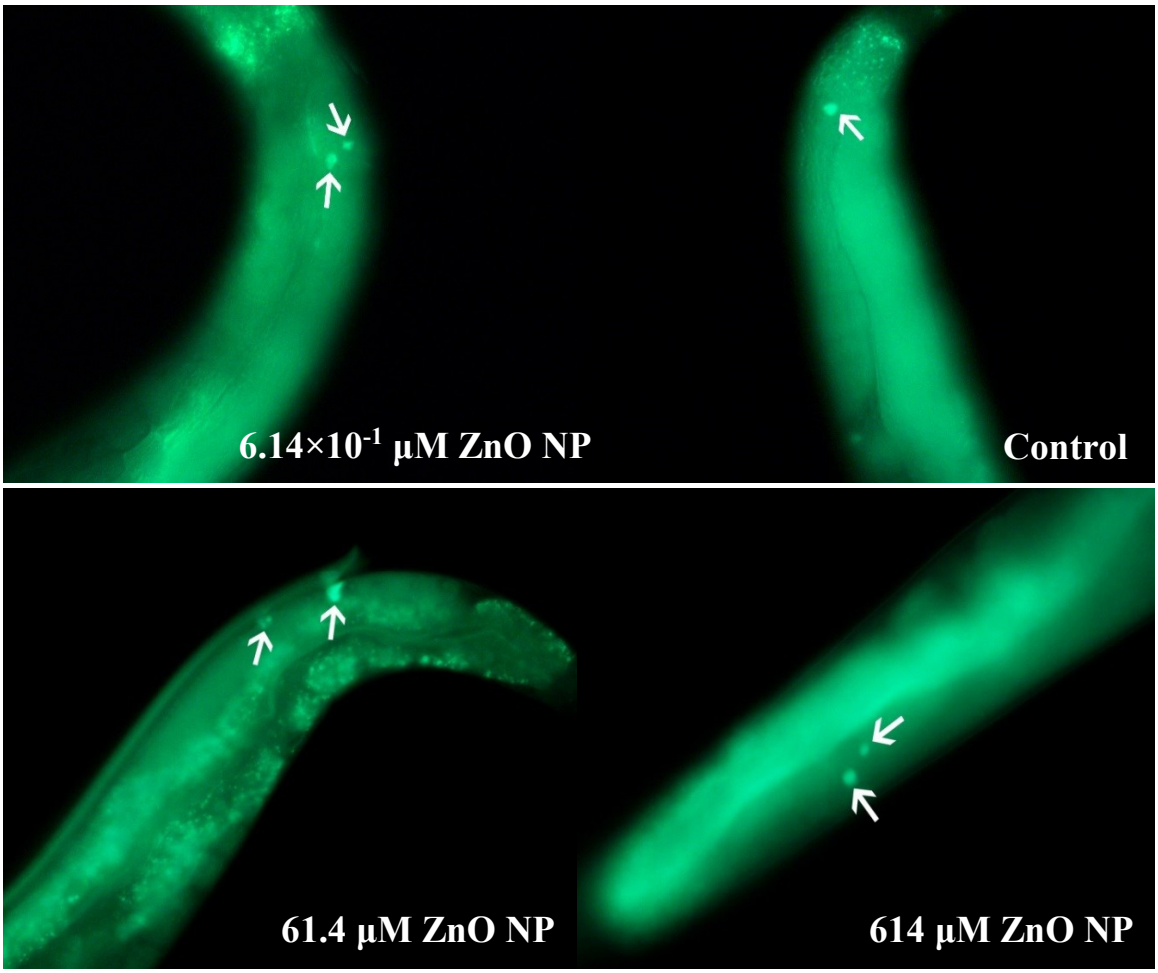

Fig. 14. ZnO NP (72 hr dose). SYTO 12 assay. Apoptotic cells appear as solid green dots indicated by white arrows. TJ-1 strain.

Gene Expression

ZnO NP Treatments

There are 13 genes involved in the main apoptosis pathway in *C. elegans* (*ced-13, ced-3, ced-4, ced-9, cep-1, dp-1, efl-1, efl-2, egl-1, egl-38, lin-35, pax-2, sir-2.1*) (Fig. 3b; Table 1). The core apoptotic machinery involved in the apoptosis process are *ced-9*, *ced-4*, and *ced-3*. As described earlier, the other 10 genes work to either inhibit or promote

regulation of these 3 core genes. *Ced-9* is an apoptosis inhibitor, while *ced-4* and *ced-3* promote apoptosis. In the 614 µM treatment, *cep-1*, *egl-1*, *lin-35*, *efl-2* and *sir-2.1* were all significantly disregulated compared to the control ($p<0.05$) (Fig. 15). In the 61.4 µM treatment there was no statistically significant difference compared to the control. In the 6.14×10^{-1} µM treatment *egl-1* was significantly up-regulated ($p<0.05$). *Egl-1*, *ced-13*, and *lin-35* are all up-regulated in both the 61.4 and the 614 µM treatments. Up-regulation of these 3 genes all reduce transcription of *ced-9* (apoptosis inhibitor) in the apoptosis pathway. *Efl-1/2*, and *dp-1* are up-regulated in all 3 treatment groups which promote the transcription of *ced-4* and *ced-3*. In the apoptosis pathway *ced-4* promotes transcription of *ced-3*, which initiates apoptosis (Fig. 3b). These results all suggest that genes respond to ZnO NP exposure by inducing apoptosis in *C. elegans*.

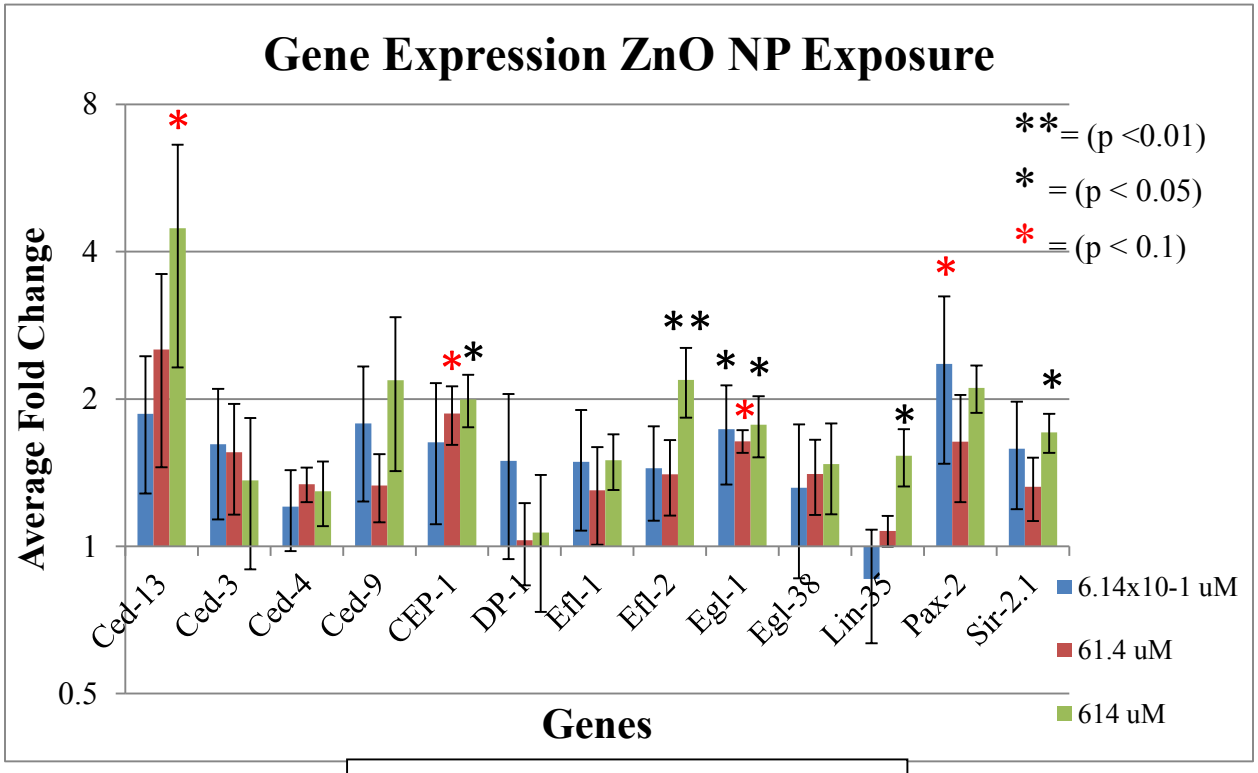

Fig. 15. qRT-PCR data. ZnO NP dose

$ZnCl_2$ Treatments

Following $ZnCl_2$ treatments, the average fold changes for all 13 tested genes are all lower than 1 fold. Only three genes, *ced-4*, *egl-38*, and *lin-35* display significant down regulations compared to control. *Ced-4* is part of the core apoptotic machinery and *lin-35* promotes physiological apoptosis, yet both were significantly down-regulated (Gartner et al., 2008). In addition, the express of *cep-1* was not changed comparing with control ($p > 0.05$).

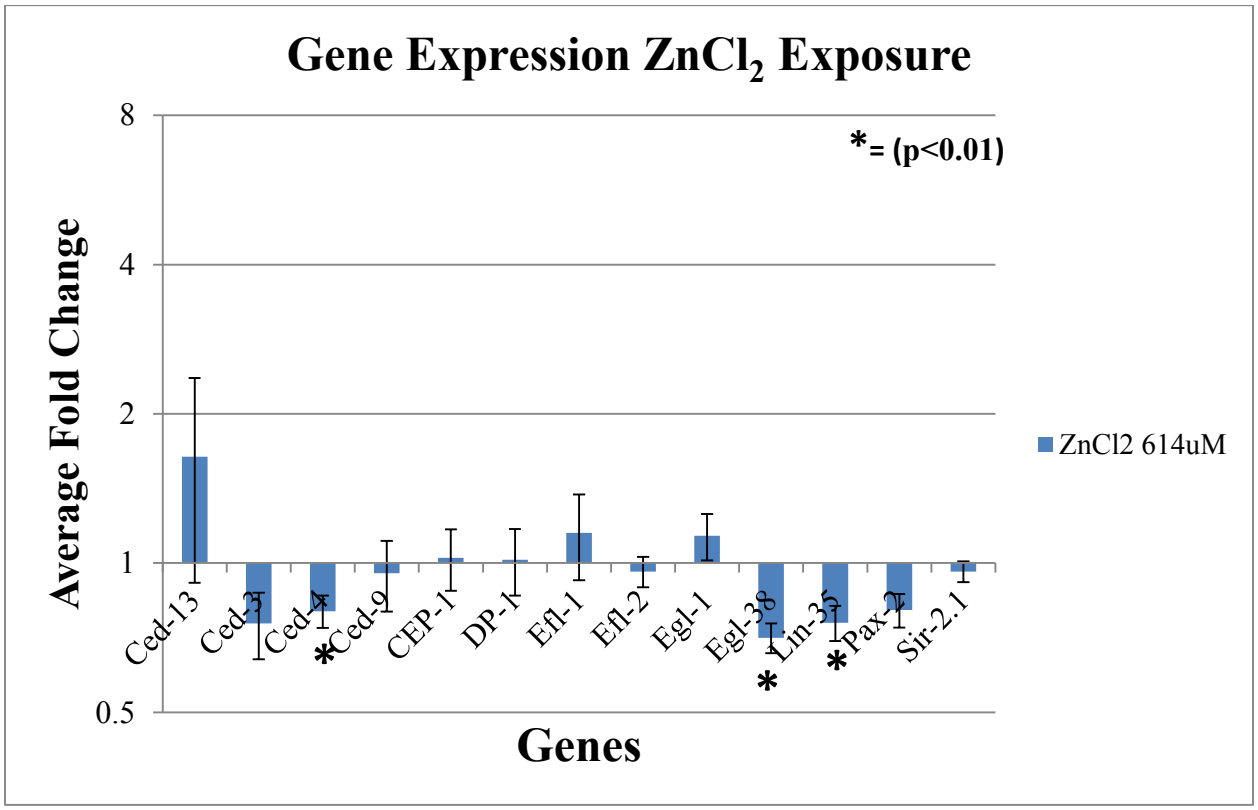

Fig. 16. qRT-PCR data. $ZnCl_2$ 24 hr dose

Microscope characterization of ZnO NPs

Using Image J software, ~400 ZnO nanoparticles total were measured from 4 different TEM images of the 61.4 µM concentration (~100 particles from each, Fig. 17

A.). The average size was determined to be 17.9±7.3 nm for the 61.4 µM concentration ZnO NPs (Fig. 18). A Malvern Zetasizer utilizing dynamic light scatter, determined the average hydrodynamic diameter of the 61.4 µM concentration ZnO nanoparticles to be 721±109.5 nm. The 614 µM concentration displayed large amounts of particle aggregates (Fig. 17 C, D).

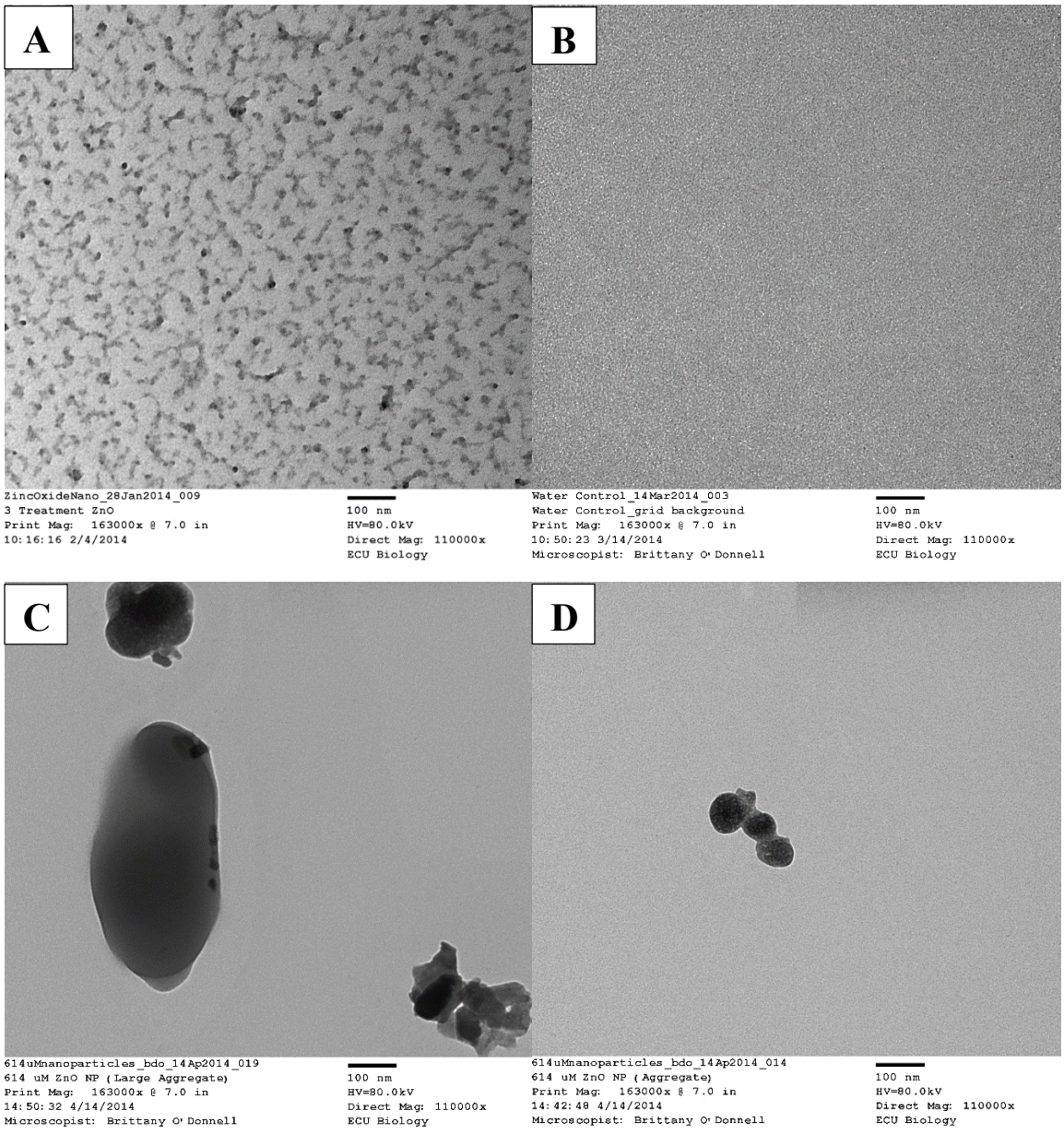

Fig. 17. A) TEM image of ZnO NPs (61.4 µM). B) Ultrapure water control. C, D) TEM images of ZnO NP aggregates (614 µM).

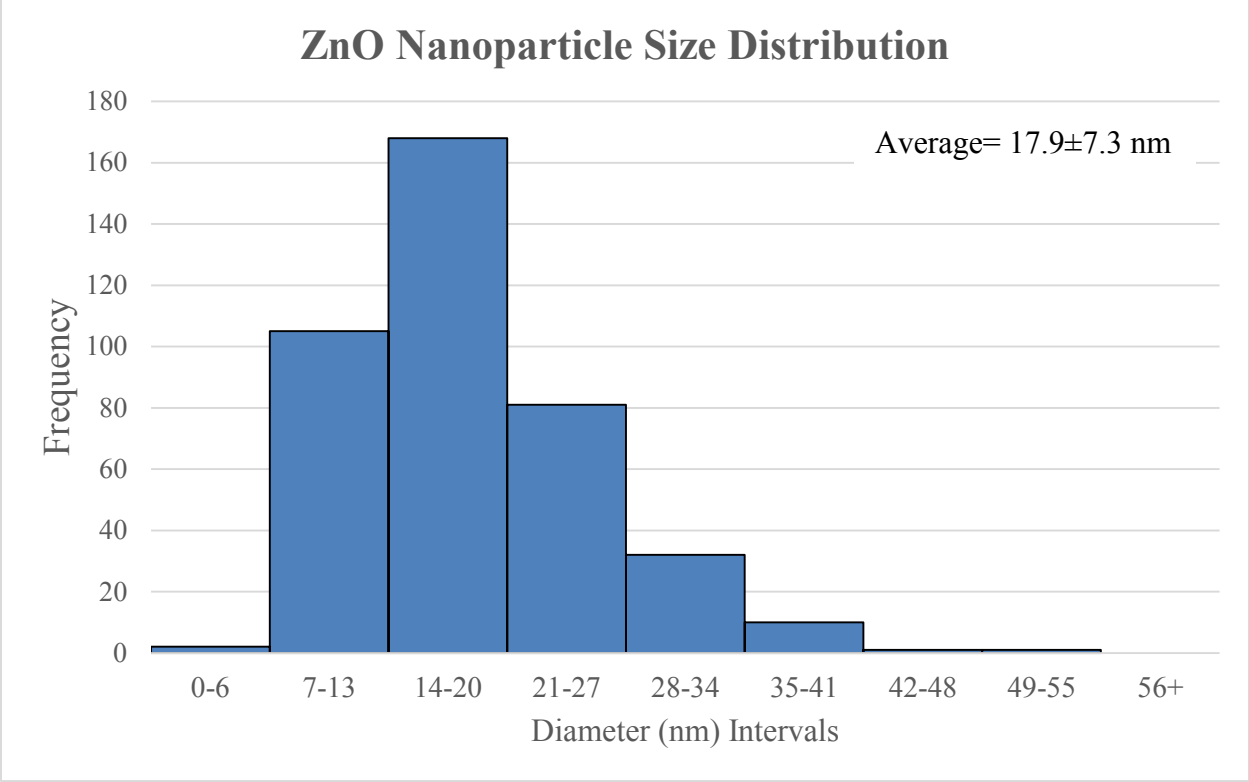

Fig. 18. Frequency histogram of ZnO nanoparticle size distribution. This information was gathered from the Image J analysis data.

TEM Imaging of ZnO Nanoparticles In vivo

N2 worms were dosed at 61.4, and 614 µM ZnO NP. Both treatment and control worms were dosed from L1 to adult stage for 72 hrs. Following fixation and staining protocol, worms were fixed, sectioned into thin 60-90 nm sections, and stained. Upon observation of the worms using the TEM, we found what could be the ZnO NPs in vivo in a 61.4 µM treatment worm. The nanoparticulate was found in the gonad region of the worm as well as under the cuticle of the worm body (Fig. 19 A, C, D). No NPs were observed in vivo in any region of the control worms (Fig. 19 B). NPs could possibly be taken up through the worm cuticle or via the ingested *E. coli* (Fig. 20).

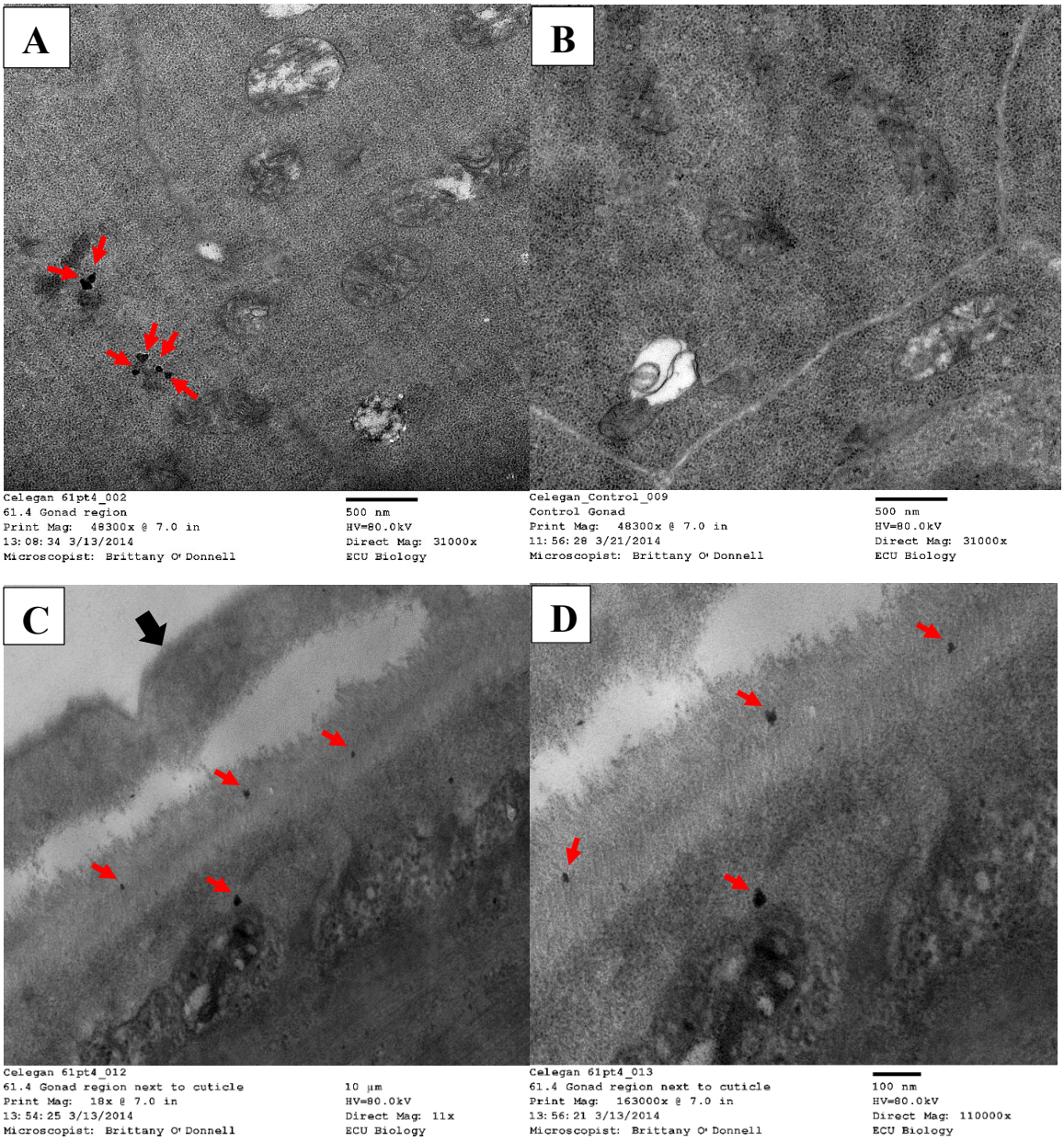

Fig. 19. (Nanoparticulate indicated by red arrows). A) TEM image of possible nanoparticulate in the gonad region of a 61.4 µM treatment worm. B) TEM image of the gonad region of a control worm with no observed nanoparticulate. C) TEM image of possible nanoparticulate under the cuticle region of a 61.4 µM treatment worm, black arrow indicates worm cuticle. D) Same as image C, but at a higher magnification.

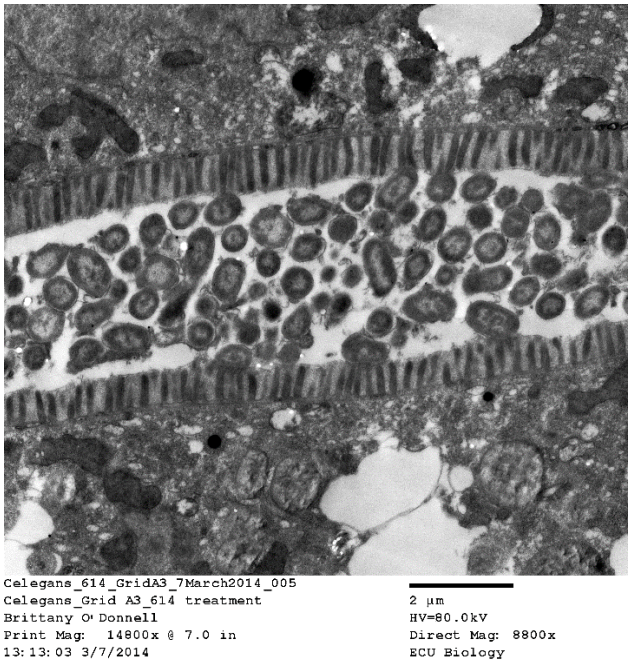

Fig. 20. TEM image of worm gut filled with *E. coli.*

DISCUSSION

SYTO 12 assay and the experiments involving the MD701 strain indicate that concentrations of 61.4 and 614 µM ZnO NPs induce germ cell apoptosis. ZnO NP induced average apoptotic cells, as observed in both MD701 and N2 strains, were nearly 2× higher in the 61.4 µM treatment compared to $ZnCl_2$ induced apoptosis at the same concentration. Average number of apoptotic cells in the 614 µM treatment was approximately the same for both ZnO NPs and $ZnCl_2$. Lower counts of apoptotic cells in the 614 µM ZnO NP treatment group may be attributed to particle aggregation (Fig. 17 C, D). The TJ-1 (CEP-1 knock-out mutant) strain was used to determine if the increase in apoptosis caused by ZnO NPs was CEP-1/p53 dependent or not. TJ-1 treatment worms,

showed no significant increase in apoptosis in any group as compared to control following ZnO NP exposure. This suggests that germline apoptosis observed in the previous ZnO NP apoptosis assays is occurring via the CEP-1/p53 dependent pathway. To investigate the genetic regulation for increased apoptosis from ZnO, we performed qRT-PCR to check gene expression of worms treated with 6.14×10^{-1}, 61.4, and 614 μM ZnO NPs. *Cep-1* was significantly up-regulated in the 614 μM treatment group. This finding supports the evidence obtained using the TJ-1 strain, that ZnO induced germ cell apoptosis is occurring via the CEP-1/p53 dependent pathway. *Cep-1* is a tumor suppressor protein which encodes for p53 in humans (Gartner et al., 2008). Apoptosis which is DNA damage related may therefore show an up-regulation of the tumor suppressor protein CEP-1/p53, as in the 614 μM treatment. According to the apoptosis pathway, results suggest that all 3 concentrations of ZnO NPs induced apoptosis, which is consistent with the fact that *egl-1*, *ced-13*, and *lin-35* were all up-regulated in both the 61.4 and the 614 μM treatments. As described earlier, in the apoptosis pathway, both EGL-1 and CED-13 interact directly with CED-9, an anti-apoptotic protein, which encodes for the cell death inhibitor BCL-2 in mammals, and inhibit its transcription, inducing the release of CED-4 and causing activation of CED-3 (caspase) (WormBase, b; WormBase, c). *Lin-35*, which was also up-regulated, encodes for Rb, the retinoblastoma protein, and promotes physiological apoptosis by inhibiting transcription of *ced-9* (Gartner et al., 2008). In addition, *efl-1/2*, and *dp-1* were up-regulated in all 3 treatment groups and as mentioned earlier, *dpl-1* encodes for Dp (dimerization partner protein) in mammals and works along with *efl-1/2*, which encodes for the transcription factor E2F in

mammals. DPL-1, Rb, and E2F seem to work together to increase CED-4 and CED-3 expression, therefore promoting physiological germ cell apoptosis (Gartner et al., 2008). $ZnCl_2$ gene expression results were very different compared to the ZnO NP data. Following $ZnCl_2$ treatments, the average fold changes, for all 13 tested genes, were all lower than 1 fold. Only three genes *ced-4*, *egl-38*, and *lin-35* displayed significant down regulations compared to control ($p<0.01$). *Ced-4* is part of the core apoptotic machinery and *lin-35* promotes physiological apoptosis, yet both were significantly down-regulated (Gartner et al., 2008). Also, the express of *cep-1* was not changed comparing with control ($p > 0.05$) (Fig. 16). In contrast, the ZnO NP gene expression data showed a significant increase in *cep-1*, suggesting that the apoptosis observed in the worms following $ZnCl_2$ exposure is likely *cep-1* independent. Overall, these findings may suggest that the core genes in apoptosis pathway were in general not changed or only marginally down-regulated under $ZnCl_2$ exposures. The apoptosis pathway was suppressed following exposure to $ZnCl_2$. In all of these experiments $ZnCl_2$ served as a comparison of effects of free Zn^{2+} to the ZnO NPs due to the fact that $ZnCl_2$ is highly soluble in water and when dissolved will create free Zn^{2+} in solution. Worms exposed to ZnO NPs had higher increases of apoptosis than worms exposed to $ZnCl_2$. Key genes in the apoptosis pathway were affected, following ZnO NP exposure, in a way that suggests that the apoptosis pathway was activated and apoptosis was induced. This was not the case for worms exposed to $ZnCl_2$. Therefore, based on the data from experiments involving $ZnCl_2$, we can conclude that the observed increased apoptosis caused by ZnO NPs was

not attributed to free Zn^{2+} alone. The NP form of Zn was found to be more toxic than the free Zn^{2+} from $ZnCl_2$.

Using the TEM, several images of 61.4 μM ZnO NPs were taken (Fig. 17 A). After analyzing ~400 various ZnO NPs using Image J software, the average size of the ZnO NPs was determined to be 17.9±7.3 nm (Fig. 18). In contrast, the average hydrodynamic diameter of the ZnO nanoparticles was determined to be 721±109.5 nm (n=30) by dynamic light scattering. The zetasizer size determination of the ZnO NPs is larger than that of the TEM method of measurement. This was the case for other studies using nanoparticles as well (Wang et al., 2009; Wu et al., 2013). Previous studies have determined the average size of the ZnO NPs to be 20nm vs. ~759nm (Wang et al., 2009) and 30nm vs. ~627±175 nm (Wu et al., 2013) for TEM vs. zetasizer measurements. Particle sizes determined by the zetasizer are measured in terms of hydrodynamic diameter, using dynamic light scattering technique. These sizes represent the sizes of NPs aggregates in aqueous solutions that mimic its environmental existence forms which was tested in this study (Wang et al., 2009). Possible ZnO nanoparticulate was observed in the 61.4 μM treatment worms in both the gonad region as well as under the cuticle region (Fig. 19 A, C, D). No nanoparticulate like objects were observed in any region of the control worms (Fig. 19 B). Observing ZnO NPs in the gonad region of the treatment worms provides evidence that the nanoparticles may possibly be taken up through the worm's cuticle or possibly via the ingested *E. coli* (Fig. 20). This also provides evidence that the NPs can reach the gonad region of the worm and thus this may contribute to the observed increases in germ cell apoptosis in the treatment worms.

GENERAL METHODS

C. elegans Treatments and Apoptosis Assays

ZnO NP suspensions were made in ultrapure water. N2 strain was synchronized and eggs were collected (Brenner, 1974) (Fig. 4) (see detailed methodology for procedure process). Eggs were allowed to hatch as L1 worms without food. N2 L1s will be kept at 20° C on an NGM agar medium with OP50 as food source. For the treatment, agar dose plates were made by mixing ZnO NP or $ZnCl_2$ solution into the agar medium to make various concentrations (6.14×10^{-1}, 61.4, 614 μM ZnO NP and $ZnCl_2$). Approximately 50 L1 stage worms were transferred to NGM agar plates for the control (unexposed worms of the same living conditions), with OP50 (*E.coli* and luria broth) as a food source. For the treatment, approximately 50 L1 stage worms were transferred onto each ZnO NP and $ZnCl_2$ dose plate with OP50 as a food source. Exposure time for both treatment and control was from the L1 to the adult stage which was ~ 72 hr. There were 3 biological replicates for each concentration of ZnO NPs and $ZnCl_2$ treatments. Following exposure worms were washed with M9 solution, transferred into microfuge tubes and a SYTO 12 assay was performed following a standard protocol (Gumienny et al., 1999) (0.75 μl of SYTO 12 in 100 μl of M9). Microfuge tubes were wrapped in aluminum foil due to light sensitivity of the SYTO dye. After 1 hour of staining microfuge tubes were centrifuged and supernatant discarded. 1 ml of PTW (1x PBS, 0.1% Tween 20) was added to the tubes, tubes were centrifuged, and supernatant discarded. Worms were transferred to fresh NGM agar plates with OP50 for 1 hour to allow the dye to exit intestines. Following the 1 hour transfer, a few worms at a time were individually placed on glass

slides with 2% agar pads and 5mM levamisole for viewing under a fluorescence microscope. Apoptotic cells were counted and recorded (Fig. 10, 11, and 12). This experiment was repeated using the TJ-1 (CEP-1 mutant) strain and ZnO NP dose plates of the same concentrations (Fig. 13, 14).

The MD701 strain was also used to determine apoptotic cell number using the exact same method as above. After synchronization worms were dosed using the same technique and method described above and dose plates were made using the same method above to make a concentration of 61.4 and 614 μM ZnO NP with 3 biological replicates. For the control, approximately 50 worms were used. For the treatment approximately 50 worms were transferred to each 61.4 μM and 614 μM ZnO NP dose plate. Worms were dosed from L1 to adult stage. These worms incorporate the GFP gene on *ced-1* and therefore do not require a staining procedure. After dosing worms were transferred to microscope slides with agar pads and levamisole for viewing. Engulfments were counted and recorded for each worm (Fig. 7, 8). This experiment using the MD701 strain was repeated once more using $ZnCl_2$ (Zn^{2+}) which serves as a comparison of toxicity with ZnO NPs (Fig. 7, 9).

Gene Expression

For gene expression, there were 5 biological replicates each group. Five NGM plates were made and over 2,000 L1 worms were plated onto each plate. Dosing plates described above were made (6.14×10^{-1} μM ZnO NP) and over 2,000 L1 worms were plated onto each plate. Both treatment and control plates were incubated at 20 °C for ~ 65 to 72 hours (L1-early adult). Each plate was then washed several times into respected

15ml falcon tubes. The tubes were centrifuged and washed with M9 3×. After washing and centrifuging, supernatant was discarded and worm pellets were transferred into microfuge tubes. Tubes were then centrifuged, supernatant discarded, and the final worm pellets were frozen using liquid nitrogen and stored in a -80°C freezer until time for RNA extractions. RNA extractions were performed (see detailed methodology for procedure process) on each of the 10 frozen tubes of worms (5 controls and 5 treatments). RNA quality of each tube was measured using a Nanodrop machine and based on results I chose the 4 best control tubes and the 4 best treatment tubes. Next, I performed reverse transcription (see detailed methodology for procedure process) and quantitative real time polymerase chain reaction (qRT-PCR) (see detailed methodology for procedure process) on the 8 remaining tubes. This experiment was repeated using the same method described above, using different dose concentrations for the treatment (61.4 μM and 614 μM ZnO NP) and a different incubation/exposure time (24 hours) (Fig. 15). This gene expression experiment was repeated once more using $ZnCl_2$ (614 μM Zn), exposure time was 24 hours (Fig. 16).

DETAILED METHODOLOGY

Synchronization Process

The synchronization and collection process is as follows, NGM plates containing the N2 worms were washed 4x with M9 solution and the worms in the M9 were transferred into 15 ml centrifuge tubes. These tubes were centrifuged, supernatant discarded, and 5 ml M9 added, then centrifuged again. This step was repeated 2 more times to wash the worms. After the third wash the supernatant was discarded, 5 ml of

synchronization solution (NaOH and bleach) was added, and tubes were gently hand shaken for approximately 5 minutes. Tubes were then centrifuged, supernatant discarded, 5 ml of M9 added, and tubes centrifuged again. The synchronization process will split open and degrade all of the worms, killing them, and leaving behind eggs that were both inside and outside of the body to be collected (Fig. 4). The remaining eggs inside the tubes with M9 will be incubated at 20° C on a shaker for approximately 16 hours, where they will hatch as L1s.

RNA Extraction

RNA was extracted using a mirVANA miRNA isolation Kit. To begin, each of the 10 frozen tubes containing all the worms were thawed on ice for approximately 10 minutes. 600 µl of Lysis/Binding Buffer was added to all 10 tubes and each tube was sonicated, to disrupt and homogenize the tissue, using an ultrasonic converter on ice. Following sonication, 60 µl of miRNA homogenate additive was added to each tube and each tube was vortexed for 30 seconds and placed on ice for 10 minutes. After ice incubation, each tube received 600 µl of Acid-Phenol Chloroform then vortexed for 60 seconds. Tubes were then centrifuged for 5 minutes (10.000 rpm) and the aqueous phase of each tube was transferred into 10 new 2 ml centrifuge tubes (this process was repeated X2). The final aqueous phase of each tube was transferred into a new tube and 1.25 volume of 100% ethanol was then added to each tube. Each of the lysate/ethanol mixtures were then transferred to filter cartridges in new tubes and centrifuged for ~15 seconds (10,000 rpm). Each filter cartridge of each tube was then washed with miRNA wash solution 1 and 2/3 provided in kit. Next, each filter cartridge of each tube was transferred

into new tubes and 50 µl of pre-heated (95°C) nuclease-free water was applied to each filter. Each tube containing filter cartridges were then centrifuged for 5 seconds (5,000 rpm) to recover RNA product. Finally, each RNA product was quantified using a NanoDrop ND-100 spectrophotometer and immediately stored in the -80 ºC freezer until time for reverse transcription.

Reverse Transcription (RT-PCR)

After NanoDrop analysis of the RNA samples, I chose the 4 best treatment and 4 best control RNA samples to use for RT-PCR (8 tubes). RT-PCR was performed using a TaqMan® MicroRNA Reverse Transcription Kit. 8 new 0.5 ml microfuge tubes were collected. Several calculations were made to determine how much nuclease free water, RNA sample, and master mix would be added to each the microfuge tubes. The master mix contained calculated volumes of components provided by the kit (RNase inhibitor, 100 mM dNTPs, 10X Reverse Transcription Buffer, Multiscribe™ Reverse Transcriptase, and primer mix (not provided in kit)). After each tube received calculated volumes of nuclease-free water, RNA sample, and the master mix, the tubes were mixed gently and centrifuged for 10 seconds (200 rpm). The tubes were then incubated on ice for 5 minutes and loaded into the thermal cycler for reverse transcription. The thermal cycler process includes 30 minutes at 16°C, 30 minutes at 42°C, 5 minutes at 85°C, and will hold at 4°C. After RT-PCR, each tube, now containing RT product or cDNA, was removed from the thermal cycler and each tube received 80 µl of DNase-free water. The tubes were then mixed by vortexing and immediately stored at -20°C until needed for qRT-PCR.

Quantitative Real-Time PCR (qRT-PCR)

To perform qRT-PCR I first placed my previously made RT-PCR products and purchased SYBR® Green dye on ice to thaw. Using a 384-well plate microplate, following a written template, I loaded each individual well with 5.5 µl RNase DNase-free water, 7.5 µl SYBR® Green dye, and 1 µl RT-PCR product. I then loaded each well with 1 µl of primer solution (20 µl forward, 20 µl reverse, 60 µl water) specific to the genes of interest. For each RT-PCR product there were 3 technical replicates. Once the plate was fully loaded it was covered and sealed tightly with a film to prevent evaporation of any well samples. The plate was then centrifuged to ensure each sample mixture is settled on the bottom of each well. Next, the plate was loaded into the qRT-PCR machine to undergo one 10 minute cycle at 95°C (enzyme activation), and 45 PCR cycles including 15 secconds at 95°C (denaturation of DNA), and 60 seconds at 60°C (DNA annealing and extension).

REFERENCES

Bailly, A., & Gartner, A. (2013). Germ cell apoptosis and DNA damage responses. *Advances in Experimental Medicine and Biology, 757*, 249-276. doi:10.1007/978-1-4614-4015-4_9 [doi]

Boxem, M., & van den Heuvel, S. (2002). C. elegans class B synthetic multivulva genes act in G(1) regulation. *Current Biology : CB, 12*(11), 906-911. doi:S0960982202008448 [pii]

Brenner, S. (1974). The genetics of caenorhabditis elegans. *Genetics, 77*(1), 71-94.

Brodigan, T. M., Liu, J., Park, M., Kipreos, E. T., & Krause, M. (2003). Cyclin E expression during development in caenorhabditis elegans. *Developmental Biology, 254*(1), 102-115. doi:S0012160602000325 [pii]

Ceol, C. J., & Horvitz, H. R. (2001). Dpl-1 DP and efl-1 E2F act with lin-35 rb to antagonize ras signaling in C. elegans vulval development. *Molecular Cell, 7*(3), 461-473. doi:S1097-2765(01)00194-0 [pii]

Chamberlin, H. M., Palmer, R. E., Newman, A. P., Sternberg, P. W., Baillie, D. L., & Thomas, J. H. (1997). The PAX gene egl-38 mediates developmental patterning in caenorhabditis elegans. *Development (Cambridge, England), 124*(20), 3919-3928.

Chi, W., & Reinke, V. (2009). DPL-1 (DP) acts in the germ line to coordinate ovulation and fertilization in C. elegans. *Mechanisms of Development, 126*(5-6), 406-416. doi:10.1016/j.mod.2009.01.008 [doi]

Denning, D. P., Hatch, V., & Horvitz, H. R. (2013). Both the caspase CSP-1 and a caspase-independent pathway promote programmed cell death in parallel to the canonical pathway for apoptosis in caenorhabditis elegans. *PLoS Genetics, 9*(3), e1003341. doi:10.1371/journal.pgen.1003341 [doi]

Derry, W. B., Putzke, A. P., & Rothman, J. H. (2001). Caenorhabditis elegans p53: Role in apoptosis, meiosis, and stress resistance. *Science (New York, N.Y.), 294*(5542), 591-595. doi:10.1126/science.1065486 [doi]

Gartner, A., Boag, P. R., & Blackwell, T. K. (2008). Germline survival and apoptosis. *WormBook, Ed. the C. Elegans Research Community,* , September, 2013. doi:doi/10.1895/wormbook.1.145.1

Gumienny, T. L., Lambie, E., Hartwieg, E., Horvitz, H. R., & Hengartner, M. O. (1999). Genetic control of programmed cell death in the caenorhabditis elegans hermaphrodite germline. *Development (Cambridge, England), 126*(5), 1011-1022.

Hall, D., & Altun, Z. (2008). *C. elegans atlas*. Cold Spring Harbor, N. Y.: Cold Spring Harbor Laboratory Press.

Hengartner, M. O. (1997). Genetic control of programmed cell death and aging in the nematode caenorhabditis elegans. *Experimental Gerontology, 32*(4-5), 363-374. doi:S0531-5565(96)00167-2 [pii]

Kenyon, C. J. (2010). The genetics of ageing. *Nature, 464*(7288), 504-512. doi:10.1038/nature08980 [doi]

Leung, M. C., Williams, P. L., Benedetto, A., Au, C., Helmcke, K. J., Aschner, M., & Meyer, J. N. (2008). Caenorhabditis elegans: An emerging model in biomedical and environmental toxicology. *Toxicological Sciences : An Official Journal of the Society of Toxicology, 106*(1), 5-28. doi:10.1093/toxsci/kfn121 [doi]

Ludewig, A. H., Izrayelit, Y., Park, D., Malik, R. U., Zimmermann, A., Mahanti, P., . . . Schroeder, F. C. (2013). Pheromone sensing regulates caenorhabditis elegans lifespan and stress resistance via the deacetylase SIR-2.1. *Proceedings of the National Academy of Sciences of the United States of America, 110*(14), 5522-5527. doi:10.1073/pnas.1214467110 [doi]

Ma, H., Bertsch, P. M., Glenn, T. C., Kabengi, N. J., & Williams, P. L. (2009). Toxicity of manufactured zinc oxide nanoparticles in the nematode caenorhabditis elegans. *Environmental Toxicology and Chemistry / SETAC, 28*(6), 1324-1330. doi:10.1897/08-262.1 [doi]

Ma, H., Kabengi, N. J., Bertsch, P. M., Unrine, J. M., Glenn, T. C., & Williams, P. L. (2011). Comparative phototoxicity of nanoparticulate and bulk ZnO to a free-living nematode caenorhabditis elegans: The importance of illumination mode and primary particle size. *Environmental Pollution, 159*(6), 1473-1480. doi:http://dx.doi.org/10.1016/j.envpol.2011.03.013

Park, D., Jia, H., Rajakumar, V., & Chamberlin, H. M. (2006). Pax2/5/8 proteins promote cell survival in C. elegans. *Development (Cambridge, England), 133*(21), 4193-4202. doi:dev.02614 [pii]

Pourkarimi, E., Greiss, S., & Gartner, A. (2012). Evidence that CED-9/Bcl2 and CED-4/apaf-1 localization is not consistent with the current model for C. elegans apoptosis induction. *Cell Death and Differentiation, 19*(3), 406-415. doi:10.1038/cdd.2011.104 [doi]

Ruan, Q. L., Ju, J. J., Li, Y. H., Li, X. B., Liu, R., Liang, G. Y., . . . Yin, L. H. (2012). Chlorpyrifos exposure reduces reproductive capacity owing to a damaging effect on gametogenesis in the nematode caenorhabditis elegans. *Journal of Applied Toxicology : JAT, 32*(7), 527-535. doi:10.1002/jat.1783 [doi]

SCENIHR (Scientific Committee on Emerging and Newly-Identified Health Risks). (21-22 June 2007). The appropriateness of the risk assessment methodology in accordance with the technical guidance documents for new and existing substances for assessing the risks of nanomaterials.

Schumacher, B., Schertel, C., Wittenburg, N., Tuck, S., Mitani, S., Gartner, A., . . . Shaham, S. (2005). C. elegans ced-13 can promote apoptosis and is induced in response to DNA damage. *Cell Death and Differentiation, 12*(2), 153-161. doi:4401539 [pii]

Shaham, S., & ed. (January 2, 2006). WormBook: Methods in cell biology., September 2013. doi:doi/10.1895/wormbook.1.49.1

U.S. Environmental Protection Agency. (2005 Office of Research and Development, Washington, DC). Nanotechnology and the environment: Applications and implications progress review workshop III.

Wang, H., Wick, R. L., & Xing, B. (2009). Toxicity of nanoparticulate and bulk ZnO, Al2O3 and TiO2 to the nematode caenorhabditis elegans. *Environmental Pollution (Barking, Essex : 1987), 157*(4), 1171-1177. doi:10.1016/j.envpol.2008.11.004 [doi]

WormBase. (a). Retrieved September/15, 2013, from http://www.wormbase.org/db/get?name=WBGene00000467;class=gene

WormBase. (b). Retrieved September/15, 2013, from http://www.wormbase.org/db/get?name=WBGene00001170;class=gene

WormBase. (c). Retrieved September/15, 2013, from http://www.wormbase.org/db/get?name=WBGene00000423;class=gene

Wu, Q., Nouara, A., Li, Y., Zhang, M., Wang, W., Tang, M., . . . Wang, D. (2013). Comparison of toxicities from three metal oxide nanoparticles at environmental relevant concentrations in nematode caenorhabditis elegans. *Chemosphere, 90*(3), 1123-1131. doi:http://dx.doi.org/10.1016/j.chemosphere.2012.09.019

Zou, H., Henzel, W. J., Liu, X., Lutschg, A., & Wang, X. (1997). Apaf-1, a human protein homologous to C. elegans CED-4, participates in cytochrome c-dependent activation of caspase-3. *Cell, 90*(3), 405-413. doi:S0092-8674(00)80501-2 [pii]